9-9-2016 12:00 AM

The Long Non-coding RNA Malat1 Regulates Inflammatory Cytokine Production in Chronic Diabetic Complications

Andrew D. Gordon, *The University of Western Ontario*

Supervisor: Dr. Subrata Chakrabarti, *The University of Western Ontario*

A thesis submitted in partial fulfillment of the requirements for the Master of Science degree in Pathology

Abstract

We examined the role of MALAT1, a highly conserved nuclear lncRNA, in chronic diabetic complications affecting the heart and kidneys, specifically with respect to inflammatory cytokine production. Endothelial cells, exposed to various glucose levels, and MALAT1 knockout mice and controls, with or without streptozotocin-induced diabetes were examined. Endothelial cells cultured with high glucose, and renal and cardiac tissue from diabetic mice showed increased inflammatory cytokine (eg. IL-6, IL-1β, TNFα) production along with transient MALAT1 upregulation. This was confirmed by both transcript and protein analyses, and such changes were prevented in the MALAT1 knockout diabetic animals. In the MALAT1 knockout animals, diabetes-induced cardiac dysfunction was also prevented. We further identified that such actions of MALAT1 are mediated by specific downstream molecules including SAA3 and p53. The data from this study provided direct evidence to the importance of MALAT1 in the pathogenesis of chronic diabetic complications involving the heart and kidneys.

Keywords

MALAT1, Long non-coding RNA, Non-coding RNA, Diabetes, Inflammation, Endothelial cells, Animal model.

Acknowledgments

I would like to express my sincerest thanks to Dr. Chakrabarti who granted me the opportunity to work in his lab. I could not have imagined a more well suited and interesting topic for me than MALAT1 and the focus we took in its involvement in inflammatory processes in diabetic complications. I am extremely grateful for both the chance to learn and grow as a scientist, and for the support, you have provided along the way.

My co-supervisor Dr. Parapuram and advisor Dr. Hardy, you have been a tremendous help in this process and I greatly appreciate the time and effort you have provided during the process.

I would also like to thank the current and past lab members Francis, Charlie, Anu, Ana, Peter, and Saumik who have helped me along in the project and were a pleasure to work alongside.

Table of Contents

List of Abbreviations

Abbreviation	Explanation
ACr	**Albumin: Creatinine ratio**
ACTB	**Beta actin**
BLAST	**Basic local alignment search tool**
CSF	**Codon substitution frequency**
CpG	**Cytosine – phosphate – guanine**
DAMP	**Danger associated molecular pattern**
Dia	**Diabetic**
DNMT	**DNA methyltransferase**
EC	**Endothelial cells**
ECM	**Extracellular matrix**
EZH2	**Enhancer of zeste 2**
FISH	**Fluorescent in situ hybridization**
H3K9me3	**Histone 3 lysine 9 tri-methylation**
HG	**High glucose**
HREC	**Human retinal endothelial cells**
HUVEC	**Human umbilical vein endothelial cells**
IL-1B	**Interleukin-1 Beta**
IL-6	**Interleukin-6**

IL-18	**Interleukin-18**
INFY	**Interferon gamma**
IRF3	**Interferon regulatory factor 3**
KO	**Knockout**
LncRNA	**Long non-coding RNA**
MALAT1	**Metastasis associated lung adenocarcinoma transcript 1**
MCP1	**Monocyte chemoattractant protein 1**
mascRNA	**MALAT1 associated small cytoplasmic RNA**
miRNA	**Micro RNA**
NEAT1	**Nuclear enriched abundant transcript 1**
NFKB	**Nuclear factor kappa B**
NG	**Normal glucose**
NLR	**Nod-like receptor**
ORF	**Open reading frame**
piRNA	**Piwi interacting RNA**
qPCR	**Real-time polymerase chain reaction**
ROS	**Reactive oxygen species**
RT	**Reverse transcriptase**
SAA3	**Serum Amyloid A 3**
SEM	**Standard error of mean**

siRNA	**Short interfering RNA**
STZ	**Streptozotocin**
TGF-B	**Transforming growth factor B**
TNFA	**Tumour Necrosis Factor Alpha**
TLR	**Toll-like receptor**
tRNA	**Transfer RNA**
WT	**Wildtype**
VEGF	**Vascular endothelial growth factor**
WT	**Wildtype**

List of Tables

List of Figures

Chapter 1

1 Introduction

1.1 Diabetes Mellitus

Diabetes mellitus is a chronic metabolic disease characterized by insulin deficiency. The disease is divided into one of two broader subcategories, type 1 diabetes and type 2 diabetes. Type 1 diabetes results from absolute insulin deficiency due to specific auto-immune destruction of the pancreatic β-cells; therefore, the body loses the ability to create and secrete insulin [1]. This is also classified as a type IV hypersensitivity reaction as the autoimmune destruction is T-cell mediated [2]. In type 2 diabetes, there is no loss of β -cells, but rather through poorly characterized mechanisms, patients develop a resistance to their body's insulin in important glucose-uptake organs such as the liver, adipose, and skeletal muscle. Whether through destruction of islets in type 1, or resistance to insulin in type 2, hyperglycemia results in diabetes through inadequate glucose uptake into the tissues leading to excessive glucose in the circulation, which leads to cellular damage. This chronic disease is both initiated and propagated by inflammatory cells and cytokines which are elevated and sustained at a low-grade throughout the disease [3]. Endothelial cells (ECs) are the principal cell type affected by hyperglycemia due to their protective barrier function [4].

1.1.1 Epidemiology

Diabetes mellitus is one of the fastest-growing health issues in the world, affecting around 400 million people worldwide, and is the seventh leading cause of death in the USA [5].The incidence of diabetes increases with the obesity epidemic and is very serious due to the increased risk for cardiovascular events, and the poor response to interventions. It is also a tremendous burden on the healthcare system where it consumes 1of every 12 global health care dollars spent [6]. As a result of hyperglycemia in both

type 1 and in type 2 diabetes, end-organ damage leads to significant mortality and morbidity in the diabetic populations. Such end organ damage leads to afflictions of the retina, kidneys, heart, and large blood vessels [7,8].

1.2 Diabetic Complications

Diabetic complications lead to functional and structural alterations through defects that arise due to chronic hyperglycemia. Diabetic complications arise in most individuals with diabetes, the complications themselves varying in degrees of severity [9,10]. Complications tend to occur later in the patient's life due to the slow progression of diabetes; however, complications can cause significant morbidity as well as mortality. This thesis focuses on the major complications affecting the eye, kidney and heart.

1.2.1 Pathogenetic Mechanism

Despite the great differences and various tissues these complications affect, diabetic complications stem from the same pathways, beginning with hyperglycemia and oxidative stress. The four well studied pathways are the Hexosamine, Protein Kinase C, AGE (Advanced Glycation End Products), and Polyol pathways [11,12]. Each of these pathways culminates in an increase in oxygen radicals, which lead to oxidative stress. These pathways lead to an increase in pro-inflammatory molecules such as tumor necrosis factor alpha (TNFα), interleukin-six (IL-6), and interleukin eighteen (IL-18) [13,14]. While each of these pathways and the inflammatory molecules have all been studied in great detail in the context of diabetes, there is a knowledge gap in their respective regulatory roles in the nucleus; therefore, understanding such processes could provide novel insight into the progression of low grade chronic inflammation in diabetes.

The four pathways mentioned above are responsible for a dysregulation of the mitochondrial electron transport chain and a subsequent overproduction of superoxide and reactive oxygen species (ROS) [15]. Oxidative stress leads to endothelial dysfunction that is a key development in diabetic microvascular disease [16]. This oxidative stress is

the direct result of hyperglycemia, which greatly influences normal transfer of protons in the mitochondria. Due to excess glucose going through glycolysis, and the formation of pyruvate NADH and $FADH_2$, the voltage across the inner mitochondrial membrane increases which blocks electron transfer from complex III [17]. The overcharged membrane stops pumping creating a halt in normal electron transport chain that leads to molecular oxygen only accepting one electron from Coenzyme Q and the formation of an O^- anion [17.18]. This generates ROS at elevated levels and can lead to cell toxicity or destruction of macromolecules. Very high levels of radical species can lead to DNA damage and an increase in cell death in susceptible cells and tissues [19].

The presence of oxygen radicals also acts as a danger associated molecule pattern (DAMP) which can be detected by innate immune receptors such as Toll-like receptors (TLRs), and Nod-like receptors (NLRs) [20]. When activated, these receptors signal to downstream transcription factors that increase production of inflammatory cytokines and related proteins. The production of ROS in a single cell triggers the activation of internal TLRs and NLRs. The activation of these receptors signals to downstream pathways including interferon regulatory factor 3 (IRF3) and nuclear factor kappa B (NFκB) which both translocate in to the nucleus and act as transcription factors for inflammatory genes. This transcription leads to increased production and excretion of molecules like TNFα, IL-6, and IL-1β, which influence development of inflammatory cells and promote a pro-inflammatory environment.

1.2.2 Diabetic Nephropathy

Diabetic nephropathy leads to functional and structural alterations of the kidney through a variety of metabolic defects. At the transcriptional level damaged cells produce vasoactive and fibrogenic factors changing renal structure and function and ultimately to renal failure [21]. Diabetic nephropathy is the leading cause of renal failure in the western world [22]. Microalbuminuria is an early manifestation in diabetic nephropathy and leads to damage to glomeruli as well as hyperfiltration [23,24]. Later, patients develop increasing proteinuria, reduced glomerular filtration rate and renal failure. As in

all diabetic complications, hyperglycemia is the most important factor leading to diabetic nephropathy [21,24]. Hyperglycemia causes multiple metabolic defects which are exacerbated by oxidative stress [21,24]. Glucose-induced EC dysfunctions result in increased production of vasoactive factors, inflammatory mediators and extracellular matrix (ECM) proteins [21,23,24].

1.2.3 Diabetic Retinopathy

Diabetic retinopathy is the leading cause of blindness in individuals under age 65 [9]. Likely as a result of the microvasculature of the eye, diabetic retinopathy is the most commonly seen manifestation of diabetic microvasculature disease. Because of this, more than 60 percent of diabetic individuals manifest some complication of damage of the retina as a result of hyperglycemia. Diabetic retinopathy manifests in progressive stages: Preclinical, non-proliferative, and proliferative retinopathy, each stage ranging from mild to severe. Preclinical retinopathy is characterized by basement membrane thickening, pericyte and EC loss [9,11,12,25]. Non-proliferative retinopathy is characterized by venous dilatation, beading, hemorrhages and exudates, capillary non-perfusion, and intra-retinal microvascular abnormalities [26]. Proliferative retinopathy is characterized by neovascularization leading to retinal hemorrhages and retinal detachment [9,25,27]. Current therapies for retinopathy include anti-vascular endothelial growth factor (VEGF) drugs as well as laser photocoagulation and burning of the blood vessels [28].

1.2.4 Diabetic Heart Disease

Cardiac complications account for the majority of diabetes related deaths [29]. Consequences related to cardiac affliction in diabetes include coronary atherosclerosis, diabetic cardiomyopathy and autonomic neuropathy [30]. Coronary atherosclerosis involves the narrowing of medium sized arteries due to the accumulation of plaque in the intimal layer. Diabetics are more susceptible to atherosclerosis due to endothelial dysfunction, which decreases nitric oxide production, as well as low-grade inflammation

in the tissues that leads to increased levels of inflammatory cytokines like TNF-α and IL-6 [31]. This alteration of the macrovasculature leads to ischemia and necrosis of the heart tissue [32].

Autonomic diabetic neuropathy results from afflictions of the small vessels. Impaired blood flow regulation in small capillary vascular beds decreases oxygen received by tissues such as the heart and integumentary system. These individuals are more susceptible for sudden cardiac death due to poor tissue perfusion [29,30]. Cardiomyopathy is a disease of the myocardium in patients with diabetes which is not explained by coronary atherosclerosis. Rather, the complication is hallmarked by impairment of the myocardial contractile properties, cardiomyocyte hypertrophy, interstitial and perivascular fibrosis, myocyte necrosis and microangiopathic lesions such as capillary basement membrane thickening [33].

1.2.5 Regulation of Gene Expression in Diabetes

Endothelial cells undergo a great number of transcriptional alterations in gene expression to compensate for changes that arise due to diabetes and hyperglycemia [11,25]. Many of these changes are attributed to oxidative stress, which is known to cause changes in cell cycle regulation and survival. Due to an increase in DNA damage from ROS, checkpoint regulator proteins are elevated to prevent mutations. P53 is such an enzyme that is elevated in diabetes and leads to an increase in apoptotic cell death should DNA repair pathways not resolve the problem. As such, proteins involved in break repair and mismatch repair are also elevated including Artemis, DNA ligase IV, and replication protein A [34,35].

Changes in gene expression are understandably accompanied by changes in chromatin organization. DNA and histones are both modified through epigenetic changes to allow for alterations in chromatin packing and accessibility to different genes [36,37]. One example of this is the loss of heterochromatin following DNA damage by oxidative

stress. Trimethylation at histone 3 lysine residue 9 (H3K9me3) is associated with decreased gene expression at that locus although the same epigenetic modification at other loci may have the opposite effect [38]. In diabetes, the loss of methylation at H3K9 leads to increased gene expression due to the loss of heterochromatin. Mice that were diabetic on a db/db background (Mice with homozygous point mutations in the leptin receptor) were found to have significantly decreased levels of H3K9me3 at inflammatory gene promoters including IL-6 and monocyte chemoattractant protein-1 (MCP1). However, the transcript and protein expression of these inflammatory cytokines were significantly increased [39].

Another common epigenetic modification is the acetylation of histones. Acetylation of lysines on histone 3 is more commonly associated with gene activation. However, to some degree this is still regulated by the specific histone acetylases and histone deacetylases, which are recruited to the site [37]. P300, a protein with a histone acetyltransferase domain was found to be expressed at significantly higher levels in cells treated with high glucose. This increase was accompanied by an elevated expression in a number of potential downstream targets including ECM proteins and angiogenic factors [40]. A separate study has also provided evidence suggesting that p300 may be involved in increased NF-κB promoter activity [41].

In addition to histones, DNA can be directly modified in diabetes either through epigenetics or through oxidative stress, leading to the formation of Hoogsteen or non-conventional base pair arrangements [42]. One common example are guanine-quadruplexes, which occur in G-rich sequences. While certain transcription factors bind with higher affinity to these structures, they also prevent proper chromatin arrangement and inhibit heterochromatin formation. This leads to changes in gene expression [42].ROS can also modify DNA through alterations in DNA methylation. DNA is primarily methylated at target cytosines in CpG dinucleotide rich regions (CpG islands) [43]. In healthy cells these CpG islands are frequently hypomethylated and lead to gene

expression; however, many of these sites are hypermethylated in diabetes leading to decreased expression of specific genes such as Sirtuin 1 (SIRT1), forkhead box P3 (FOXP3), and peroxisome proliferator-activator receptor gamma coactivator 1-alpha (PPARGC1A) [44-46]. This is likely due to their G rich regions that are conducive to forming guanine-quadruplexes as described above which greatly impair the activity of demethylases [47]. DNA methyl transferases (DNMTs) and demethylases are the enzyme classes responsible for the addition and removal of these methyl groups. Upon exposure to ROS agents such as peroxide, DMNT1 binds with stronger affinity to chromatin, specifically at CpG rich regions [48]. Furthermore, H_2O_2 treatment and damage triggers the formation of a complex including DNMT1, SIRT1, and Enhancer of zeste 2 (EZH2), which removes these proteins from their normal locations in the nucleus and further repress gene expression [49].

Micro RNAs are also frequently altered in diabetic complications and have been shown to play important roles. MiRNAs have been implicated in many relevant pathways in diabetes from fat metabolism and cholesterol synthesis to insulin secretion and immune cell recruitment [50, 51]. MiRNAs play important roles in proliferation, differentiation and cell signaling, all of which are vital processes in diseases including diabetes [52, 53]. MiR-133 has been implicated in cardiomyopathy and diabetic nephropathy after it was found to be aberrantly expressed in diabetic heart and kidney tissues [54]. MiR-200b isoform has also been implicated in both diabetic retinopathy and cardiomyopathy where it regulates VEGF [55.56]. The importance of miRNAs in diabetes is further supported by studies using Dicer, an enzyme that is required in the biogenesis of miRNAs. Mice deficient in Dicer have significant proteinuria, hyperfiltration, and damage to their glomeruli, all of which are seen in diabetic kidney disease [57,58]. Our lab has previously shown roles for multiple miRNAs in chronic diabetic complications. In this research, we focus on long non-coding RNA.

1.3 Non-Coding RNA

Most of the eukaryotic genome is transcribed yielding thousands of transcripts of varying sizes; however, the vast majority of these transcripts have no protein-coding capacity [59]. Non-coding RNAs (ncRNAs) were considered to be 'junk DNA' or ‘noise’ until recently when it was discovered that they not only make up the majority of the human genome, but many of them are highly conserved and functional [59-61]. NcRNAs are RNA molecules of any size that are transcribed from DNA, but do not undergo translation in to a stable product. In addition, many ncRNAs show cell type specific expression, complex organizational patterns, and association with human diseases [59-61]. General classes of ncRNAs include microRNA (miRNA), short interfering RNA (siRNA), piwi-interacting RNA (piRNA), and long non-coding RNA (lncRNA [62,63]. The principal ncRNAs involved in pre and post-transcriptional regulation are further sub categorized based on size. NcRNAs less than 30 nucleotides in length are termed short, those ranging from 31 to 200 nucleotides are called medium, and those of length greater than 200 nucleotides are classified as long ncRNAs [64]. All groups of ncRNAs have been shown to serve a wide variety of functions in all tissues. Such functions include heterochromatin condensing, histone modification, DNA methylation, gene silencing, and protein organization [61,65,66].

1.4 Long non-coding RNA

LnRNAs are loosely defined as any RNA molecule which is greater than 200 nucleotides and does not code for a functional protein product [67]. As such, the group is very diverse containing molecules continuing 200 nucleotides to well over 10 thousand nucleotides. Occasionally molecules once considered to be non-coding are found to code for a protein which also changes which molecules are in this group. As such, there are still well over 4000 characterized unique lncRNAs in humans that make up both the majority of the genome in percent composition of known transcripts, and total unique members compared to any other group [64]. As with most genes, lncRNAs are frequently regulated

both spatially and temporally by both the specific tissue or cell type, and the stage of development.

1.4.1 Long non-coding RNA location in genome

LncRNAs are also found all across the genome on all chromosomes and can be categorized based on their location. The five principal locational types of lncRNAs are intronic, intergenic, antisense, bidirectional, and senses lncRNAs [68]. As the name suggests, intronic lncRNAs are found in intronic regions of protein-coding genes and are produced through alternative splicing of pre-mRNA. The can be on either the sense or anti-sense strand or in the opposite direction as the protein-coding gene, but they do not overlap with the protein coding gene [69]. Intergenic lncRNAs are located in distinct transcriptional segments from coding genes. They have their own unique gene sites and are at least 10kb removed from the nearest protein coding gene [65,69]. Antisense lncRNAs are on the complementary sequence to the coding sense stand. They may overlap with coding exons but their segments are spliced together to form a non-coding product [70,71]. Bidirectional lncRNAs originate from divergent transcription from the promoter of a protein-coding gene. As a result of this, they are usually very close in proximity to, and on the opposite strand as the coding gene [69,72]. Sense lncRNAs overlap the sense strand sequence of a protein-coding gene. The lncRNA can overlap a portion of, or be entirely bound by the protein coding gene [72].

1.4.2 Long non-coding RNA Functions

In spite of their overwhelming prevalence, the functions of lncRNAs remain relatively unclear. Even in cases where functionality is known, it is highly probable that due to their sheer size they are capable of multiple diverse functions [73]. While they do not code for proteins themselves, they are able to regulate protein and non-protein coding genes through both -cis and -trans effects [74]. LncRNAs influence gene expression by

signalling and regulating gene expression, act as decoys to inhibit specific interactions, guiding proteins to specific chromatin sites, and scaffolding to organize and complex molecules in specific cellular compartments [62,64,66]. Through these mechanisms and potentially others, lncRNAs are able to influence a variety of cellular functions. However, their role in diabetic complications remains under investigated. In the following paragraphs I will discuss specific lncRNA relevant to this thesis.

1.5 MALAT1

1.5.1 Malat1 structure and conservation

MALAT1 (Metastasis associated lung adenocarcinoma transcript 1, NEAT2) was first identified in 2003 in early-stage non-small cell lung cancer cells [75]. MALAT1 is found on chromosome 11q13.1 where it encodes an 8.7 kb transcript. In mouse, it is found on chromosome 19 and is slightly smaller at 6.98 kb though nearly 5kb are identical between mouse and man and this high level of conservation is found in mammals. Regions of MALAT1 can be found as far back in evolution as frogs and fish [76,77]. In addition to not localizing to the cytoplasm, MALAT1 has no functional ORFs and lacks the ability to bind ribosomes which have added to its classification as non-coding [74,76,78].

MALAT1 is encoded on a single exon and does not undergo any significant known alterations, modifications, or splicing. The gene also encodes nearly no repeat elements. Some studies have reported that a small 61-80 nucletotide RNA molecule is cleaved and may enter the cytoplasm but remains untranslated [79,80]. This small RNA has been called MALAT1-associated small cytoplasmic RNA (mascRNA). MascRNA seems to be a likely candidate for a transfer RNA (tRNA) derived element [80]. This postulated molecule is found at 3’ end of the MALAT1 RNA, anterior to the 3’ helix motif. MALAT1 and its neighboring gene nuclear enriched abundant transcript 1 (NEAT1), have been postulated to have arisen from a duplication event in the genome due to their unique positions beside each other in the mammalian genome, and similar length [81]. However,

MALAT1 and NEAT1 share almost no sequence homology beyond a small 3’ region [77].

(lncRNA) MALAT1 is highly stable for an RNA molecule with half-lives reported between 9 and 24 hours [82]. Much of this stability is likely due to both its strict presence in the nucleus where there is less overall degradation, as well as a stable triple helix secondary motif at its 3’ terminus [68,83,84]. Because of this, there is also not ability for this RNA to be polyadenylated [83]. In addition to its unique helix motif, MALAT1 has a distinct sequence or secondary structure that allows it to localize to specific foci known as paraspeckles [66]. At these nuclear speckles, MALAT1 complexes with other molecules including its neighboring gene NEAT1 [66]. This secondary structure, along with its tremendous length, makes MALAT1 a poor target for knockdown experiments which are not sufficient to uncover a function for the lncRNA [85,86]. The gene’s expression can be verifiably eliminated with the use of multiple zinc finger nucleases [85]. Mouse knockout models of MALAT1 have been generated and are not only non-lethal, but also show no observable phenotype, including the cells’ ability to form nuclear paraspekles [66,86]. To date these models have only been used to study a small number of diseases and processes.

1.5.2 Malat1 function and interactions

MALAT1 is found at high levels in nearly all tissues and cells with some of the highest reported in the colon, liver, immune cells, kidney, lung, brain, and heart. Because of this, it remains to be seen whether MALAT1 exerts a single function in all tissues, or a tissue specific role dependent on the tissue it is in. Several functions and interactions have been found for this molecule with most of them involved in cancer, where it has been primarily studied to date.

In cancer, MALAT1 has been shown to regulate metastasis and cell motility. As such, MALAT1 had been reported to be elevated in many cancers including breast cancer, cervical cancer, colorectal cancer, liver cancer, neuroblastoma, osteosarcoma, pancreatic

cancer, prostate cancer, and gastric cancer [76,84,87,88]. In each of these cancers, MALAT1 is associated with a poor prognosis, whereby as the level of transcript increases, patient survival rate decreases [89]. Because of this MALAT1 has been termed an oncogene [88,90]. One study has also proposed that MALAT1 is involved in the alternative splicing and expression of other oncogenes [89,90]. MALAT1has also been shown to be of importance in other diseases including pre-eclampsia, ischemia, and sinoatrial node disease. One study also found elevated levels of MALAT1 in the hippocampus, cerebellum, and brainstem of human alcoholics [91].

One of the most notable proteins involved in regulation of MALAT1 is p53. One study found that when p53 was overexpressed MALAT1 levels decreased significantly [92]. A considerably enriched p53 binding locus called BS-p53-1 was also shown to be enriched in the MALAT1 promoter [92]. A separate study found a deletion of MALAT1 lead to increased activation of p53 [93]. This association is further strengthened by numerous studies that knockout or knockdown MALAT1 and report a decrease in proliferation and cell survival [89]. MALAT1 knockdown cells also show higher sensitivity to apoptosis inducing agents [89]. Together these findings suggest MALAT1 may be both regulated, and a regulator of p53. This may help to explain MALAT1's upregulation in diseases like cancer where cell death is suppressed, but its downregulation in ischemia and other disease characterized by chronic cell death.

Other functional roles for MALAT1 that have been reported include its ability to regulate TGF-β signaling via SMAD2/3 [94]. In addition, it has been shown that MALAT1 regulates serum amyloid A3 (SAA3) [95]. SAA3 stimulates IL-6 and TNFα production through NFκB. MALAT1 has also been shown to regulate its neighboring gene NEAT1 through cis interactions [66].

1.6 Rationale

Diabetic complications involve a large number of alterations to gene expression, all of which are mediated through proteins and molecules resident in the nucleus. LncRNAs are a relatively unstudied class of molecules, many of which are highly conserved and either initiate or reside in the nucleus. We identified MALAT1 in a transcript array as a non-coding RNA which is aberrantly expressed in endothelial cells under hyperglycemic stress [Figure 1]. MALAT1 is also one of the lncRNAs with the highest expression across multiple tissues in mammals and is dysregulated in multiple diseases.

Preliminary work completed by our lab showed that MALAT1 expression is elevated at specific points over a time course treatment of high glucose in endothelial cells. Furthermore, the increase in MALAT1 transcript expression correlated with increases in multiple proteins including inflammatory cytokines such as IL-6 and TNFα. Using MALAT1 specific antisense oligonucleotides, MALAT1 levels were then reduced, and this reduction correlated to a similar reduction in these inflammatory cytokines [95]. Recently, another study has confirmed this finding as well, showing that TNFα expression in splenocytes was lower in mice lacking MALAT1 compared to WT mice [96]. Based on these rationales, we developed the following hypothesis:

1.7 Hypothesis

MALAT1 is an important regulator of inflammatory cytokines in chronic diabetic complications.

1.8 Specific Aims

1. To investigate the role of MALAT1 in the production of inflammatory cytokines in endothelial cells exposed to high glucose.

2. To investigate the role of MALAT1 in the production of inflammatory cytokines and subsequent organ damage in mice with diabetes.

Chapter 2

2 Material and Methods

2.1 Animal Studies

Through collaboration with Dr. Spector (Cold Spring Harbor Laboratory, Cold Spring Harbor, New York, USA), mice were obtained that have a ~3 kb deletion in the 5' end and promoter of the MALAT1 gene [66].This homozygous deletion is a global knockout eliminating MALAT1 transcript expression in all tissues. The mice were generated on a C57/BL6 background. Diabetes was induced in 10-week old mice using 5 injections of low dose streptozotocin (STZ) (Sigma, Oakville, Ontario, Canada; 50 mg/Kg IP, Na Citrate buffer, pH5.6) on consecutive days, controls receiving and equal volume injection of buffer only [97]. Diabetes was evaluated based on a 4 hour fasting blood glucose level greater than 20mmol/L. Control mice had glucose levels less than 10mmol/L. Mice were all age matched and only male mice were used. The following groups of animals were used: **a)** Non-diabetic control animals, **b)** STZ induced diabetic control animals **c)** MALAT1 knockout mice, **d)** MALAT1 knockout mice with STZ- diabetes. All animals were housed with access to standard diet (Harlan 2018 rodent diet) and water *ad. Libitum.* Animals were monitored up until the time of sacrifice at either 1 week, 2 weeks, 4 weeks, or 8 weeks post diabetes. Blood glucose levels, urine ketones, and body weight were frequently recorded and monitored. Mice were euthanized by Forane™ (Baxter, Toronto, Ontario, Canada) overdose and asphyxiation. Following sacrifice, blood, kidney, heart, retina and other major organs were collected. Small portions of the tissues were snap frozen for RNA and protein analyses and the remaining tissue fixed in 10% formalin to be used for other experiments. All procedures were approved by the University's Animal Care Committee [97].

2.2 Cell Culture

Human umbilical vein endothelial cells (HUVEC) and human retinal endothelial cells (HREC) were purchased frozen from Lonza (Jackson, Wisconsin, USA), and Olaf Pharmaceuticals (Worcester, Massachusetts, USA) respectively. Cells were grown at 37C, 5% CO_2, in EBM-2 (Lonza) supplemented with 10% fetal bovine serum (FBS). Cells at passages 4, 5, and 6 were used for experiments and were plated at a density of 2,500 cells/cm^2. Once the cells had reached a confluency of 75%, they were serum starved for a 24-hour period. Following this, D-Glucose was used to stimulate cells at concentrations of 5ug/ml (Normal Glucose) or 25ug/ml (High Glucose). Cells were cultured for 6 hr, 12 hr, 24 hr, or 48 hr in the treated media before harvest for experiments [98].

2.3 RNA Isolation

Mouse tissue RNA extraction was carried out using the PureLink™ RNA Mini Kit (Ambion Life technologies, Carlsbad, California, USA) and following the manufacturer's protocol. The tissues were homogenized in Lysis buffer using either a mechanical homogenizer or a mortar and passage through a 20-gauge needle 4 times. An equal volume of 70% (v/v) ethanol was added to the homogenized tissue and then the homogenate was transferred to a spin cartridge to elute the liquid. RNA bound to the membrane of the column was washed with included buffers before eluting with molecular grade water. RNA purity and concentration were assessed with either a spectrophotometer or a nanodrop measuring at 260 and 280 nm. RNA was then immediately reverse transcribed to cDNA or kept at -70C.RNA extractions of HUVEC and HREC were carried out with TRIzol™ Reagent (Invitrogen INC, Burlington, Ontario, Canada) following the manufacturer's instructions and as previously described [98].

2.4 DNA Isolation and Gel Electrophoresis

DNA was extracted from mouse tail by a phenol-choloformextraction.A 1 cm piece of tail was digested overnight in tail buffer using protinase K heated to 45 °C. DNA was then extracted using phenol:choloform using a mixture of 25:24 (v/v). After vortexing and centrifugation at 13,000 rpm, the supernatant was collected and DNA was then precipitated via isopropanol and centrifuged again at 13,000 rpm for 10 minutes. The supernatant was removed again and the DNA pellet was then washed with 70% ethanol and spun down a final time. The ethanol was removed and any residual alcohol was left to evaporate at room temperature. DNA was then reconstituted in deionized water and stored at -20 °C to be used for genotyping. The sample purity was measured using the ratio of ultraviolet absorbance at 260 and 280 nm. The DNA concentration was determined measuring the absorbance at 260 nm.

DNA gel electrophoresis was used to validate the genetic knockout of MALAT1 in mice. Two regions of MALAT1 were first amplified by PCR using primers specific to the MALAT1 DNA sequence and flanked the cut site. DNA was amplified using TaqDNA polymerase and PCR buffer (FroggaBio; North York, Ontario, Canada). Agarose gels were prepared using 1.5% agarose in TAE buffer (10 nM Tris base, 0.5 mM EDTA, 4.4 mM acetic acid, pH 8.0). 3ul of Ethidium Bromide was added to create the gel. The wells were loaded with 10ul of sample (8 ul DNA, 2 ul Loading buffer), a 1 kb DNA ladder, or a negative control (no template). The electrophoresis was done in TAE buffer and run at 100 volts for 1.5 hours. Gels were visualized under ultraviolet light and photos were taken.

2.5 LncRNA Array

RNAs were extracted using the RNAeasy miRNA isolation kit (Qiagen, Austin, TX) according to the manufacturer's instruction. Custom analysis of lncRNA expression profiling from human retinal cells treated with high or normal glucose for 24 hours (n = 3/group) were performed by Asuragen Inc. (Austin, TX).

2.5.1 LncRNA Array Protocol

Sample labeling and array hybridization were performed according to the Agilent One-Color Microarray-Based Gene Expression Analysis protocol (Agilent Technology) with minor modifications. Briefly, mRNA was purified from total RNA after removal of rRNA (mRNA-ONLY™ Eukaryotic mRNA Isolation Kit, Epicentre). Then, each sample was amplified and transcribed into fluorescent cRNA along the entire length of the transcripts without 3' bias utilizing a mixture of oligo(dT) and random priming method (Arraystar Flash RNA Labeling Kit, Arraystar). The labeled cRNAs were purified by RNeasy Mini Kit (Qiagen). The concentration and specific activity of the labeled cRNAs (pmol Cy3/μg cRNA) were measured by NanoDrop ND-1000. 1 μg of each labeled cRNA was fragmented by adding 5 μl of 10 × Blocking Agent and 1 μl of 25 × Fragmentation Buffer, then the mixture was heated at 60 °C for 30 min, and finally 25 μl 2 × GE Hybridization buffer was added to dilute the labeled cRNA. 50μl of hybridization solution was dispensed into the gasket slide and assembled to the LncRNA expression microarray slide. The slides were incubated for 17 hours at 65 °C in an Agilent Hybridization Oven. The hybridized arrays were washed, fixed and scanned with using the Agilent DNA Microarray Scanner (part number G2505C).

2.5.2 Array Data Analysis

Agilent Feature Extraction software (version 11.0.1.1) was used to analyze acquired array images. Quantile normalization and subsequent data processing were performed using the GeneSpring GX v12.0 software package (Agilent Technologies). After quantile normalization of the raw data P/M filtration, lncRNAswere chosen for further data analysis. Hierarchical Clustering was performed using the R software (version 2.15).

2.6 RNA in Situ Hybridization

RNA Fluorescent in situ Hybridization (FISH) was carried out using specific probes and reagents designed by Stellaris™ RNA FISH (Biosearch Technologies, Petalume, California, USA).To detect MALAT1 RNA, cells which were grown on coverslips were rinsed briefly in PBS and then fixed in 2% formaldehyde in PBS for 10 mins at room temperature (RT). Cells were made permeable in 70% (vol./vol.) Ethanol diluted in DEPC treated water overnight at 4°C. Cells were washed in Wash Buffer A for 5 minutes prior to hybridization. Hybridization was carried out using Stellaris™ RNA FISH probes dissolved in TE buffer to a concentration of 12.5 uM. Hybridization buffer was then used to dilute the probe to a working concentration of 125 nM and incubated with the cells in a moist chamber at RT for 4-6 hr. For nuclear visualization, cells were rinsed with Wash Buffer A and Wash Buffer B, and nuclei were then counterstained with Hoechst Stain (5ng/mL) for 30 minutes in the dark at RT. Coverslips were then mounted on slides to be visualized by immunofluorescence [99].

2.7 cDNA synthesis and Quantitative RT-PCR

For real-time quantitative PCR (Q-PCR), first 1ug of total RNA was reverse transcribed to cDNA using High Capacity CDNA Reverse transcription Kit (Applied Biosystems Inc., Foster City, California, USA). The kit used a MultiScribe™ reverse transcriptase enzyme, as well as random oligo hexamers to amplify all RNA. Gene-specific primers sets were designed using NCBI basic local alignment program (BLAST) or ordered pre-designed from Qiagen (Toronto, Ontario, Canada), Q-PCR was carried out in duplicate using SYBR Green Master Mix (Clontech, Mountain View, California, USA) and run using a LightCycler™ 96 (RocheDiagnotstics Canada, Laval, Quebec, Canada)[5]. SYBR Green is a dye that binds to double stranded DNA and fluoresces, allowing for detection of all double stranded products in each cycle. Target genes were analyzed using standard curves to determine relative levels of gene expression. Molecular grade water was used to make up the volume difference in both the negative control, and no RT control. The levels of specific RNAs were analyzed using the Roche LightCycler™ 96 System. Individual RNA samples were normalized according to the level of β-actin [55]. All sequences for reverse and forward primers used are summarized in Table 2.1.

2.8 ELISA

Proteins were isolated from mouse tissue using radioimmunoprecipitation assay buffer. Protein concentration was then measured using a BCA protein assay kit (Pierce, Rockford, Illinois, USA). Protein concentrations were kept constant across protein lysates used for ELISA. For detection of IL-6 and INFγ in tissue homogenate, pre-coated plates were obtained from R&D systems (Minneapolis, Minnesota, USA) and the protocol was followed to the manufacturer's instructions. Plates were measured at 450 and 570 nm (to correct for plate defects) using a plate reader. For detection of albumin and creatinine in mouse urine, Albuwell™ and Creatinine Companion kits were ordered from Exocell (Philadelphia, Pennsylvania, USA) [95].

Table 2.1: Oligonucleotide sequences for Real-Time PCR

Gene	Primer sequences (5' – 3')
Hs[a]/Mus[b] ACTB	F: TGTGGATCAGCAAGCAGGAG R: TGCGCAAGTTAGGTTTTGTC
Hs MALAT1	F: TCTTAGAGGGTGGGCTTTTGTT R: CTGCATCTAGGCCATCATACTG
Hs TNFA	F: AGGCGCTCCCCAAGAAGACAG R: AGCAGGCAGAAGACGTGGTG
Hs IL6	F: GGGGCTGCTCCTGGTGTTG R: CTGAGATGCCGTCGAGGATGTA
Hs IL1B	F: GCGGCATCCAGCTACGAATCT R: GGGCAGGGAACCAGCATCTT
Mus MALAT1	F: TGGGGGAGTTGTAGGCTTCT R: GGAGTGAGGCTTGTGGTAGG
Mus NEAT1	F: TGGCCCCTTTTGTTCATTAGC R: TGGAAGGCCATTGTTTCAGG
Mus P53	F: CTCCCTTGCTGTAGGTAGCG R: CGTCGATGCAGTGAGGTGAT
Mus SAA3	F: TGACAGCCAAAGATGGGTCC R:TCCGGGCAGCATCATAGTTC
Mus TNFA	F: AGGCACTCCCCCAAAAAGAT R: CACCCCGAAGTTCAGTAGACAG
Mus IL1B	F: TTCAGGCAGGCAGTATCACTC R: GAAGGTCCACGGGAAAGACAC
Mus IL6	F: ACAACCACGGCCTTCCCTACTT R: TCATTTCCACGATTTCCCAGAG

[a]Hs, Human, [b]Mus, mouse. F, forward primer; R, reverse

2.9 Cardiac Ultrasound Imaging

Echocardiographic and Doppler studies were performed using the Vevo™ 2100 imaging system (Visualsonic, Toronto, Ontario, Canada). All data were performed 1 week prior to the time of sacrifice between 1 and 5 PM. Each mouse was anesthetized in a sealed chamber with inhalant isolfuorane at 3% in 100% oxygen. Once anesthetized, the mouse was transferred and secured on its dorsal side to a heated imaging platform and isofluorane was maintained at 1% for the duration of the experiment. The hair of the mouse chest was carefully removed, and an electrode gel was applied to the chest before placing the transducer to the left of the sternum. At this position, images were obtained of the left ventricle along its long axis. The blood flow velocity was measured using Doppler ultrasonography to directly measure the flow motion (Pulse Wave Doppler). M-mode tracings of the heart were acquired by rotating the transducer to be perpendicular to the left ventricle and aligned along the short axis of the heart. Measurements were averaged from 3 consecutive cardiac cycles [55,100].

2.10 PhyloCSF

To measure the coding potential of MALAT1 and other gene transcripts, we used the previously established codon substitution frequencies (CSF) method to evaluate the evolutionary characteristics in their alignments with orthologous regions in other sequenced mammalian genomes [101,102]. CSF generates a likelihood score for a given sequence considering all codon substitutions observed within its alignment across multiple species, which was based on the relative frequency of similar substitutions occurred in known coding and noncoding regions. CSF compares two empirical codon models; one generated from alignments of known coding regions and the other according to noncoding regions, producing a log odds likelihood ratio reflecting which model better explains the alignment. The source code and executables are freely available at http://compbio.mit.edu/PhyloCSF.

2.11 Statistical Analysis

All experimental data are expressed as mean ± SEM and were analyzed by ANOVA followed by Student's t-test. Differences are represented as significant as values of $p<0.05$.

Chapter 3

3 Results

3.1 Screening for a potential LncRNA of interest

Initially, we performed a custom microarray analysis (Arraystar) to identify lncRNA changes. To this extent, we exposed human retinal endothelial cells (HRECs) to high or normal glucose treatment for 24 hrs. MALAT1was identified as a gene, which was dysregulated in high glucose compared to normal glucose treatment. Extracted RNAs were sent for quantitation by array analysis, which was designed to detect a large number of human lncRNAs. MALAT1 was identified as one of many lncRNAs that was downregulated when HREC cells were cultured in high glucose compared to cells cultured in low glucose [Figure 3.1].

This finding from the array was then tested in HUVECs where we cultured the cells in high and low glucose. Using qRT-PCR it was found that levels of MALAT1 were significantly elevated at 48 hours of high glucose (25μM) treatment compared to cells in normal glucose (5μM) treatment [Figure 3.2]. Since MALAT1 is highly expressed in nearly all tissue types, it is likely to have tissue specific functions. Furthermore, the targets of MALAT1 included molecules of interest in the context of diabetic complications including SAA3, p53 and VEGF.. Hence, alterations in MALAT1 expression in different cell types made MALAT1 a promising candidate gene for follow up studies.

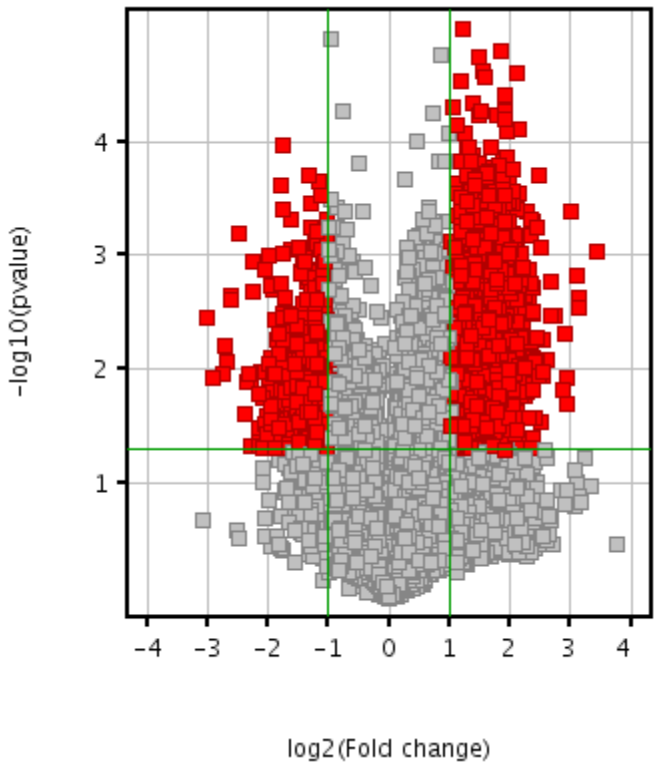

Figure 3.1: LncRNA Array Analysis

Total RNA was isolated from HRECs cultured for 24 hours in high gluose (25 mM) or normal glucose (5 mM) media and sent to Aiglent Technology. mRNA was purified from total RNA after removal of rRNA and each sample was amplified and transcribed into cRNA using a mix of oligo(dT) and random priming. cRNAs were further purified following which slides were assembled and RNA was hybridized to a lncRNA array. After incubation, slides were fixed and scanned with using the Agilent DNA Microarray Scanner. Agilent Feature Extraction software was used to analyze acquired array images. Subsequent data processing was performed using the GeneSpring GX v12.0 software package. Hierarchical Clustering was performed using the R software. Array probes were sequenced through BLAST and MALAT1 was identified as a lncRNA downregulated more than 3 fold in the HG compared to NG treated HRECs [n=3 per group, data displayed as means, data points in red indicate statistical significance.]

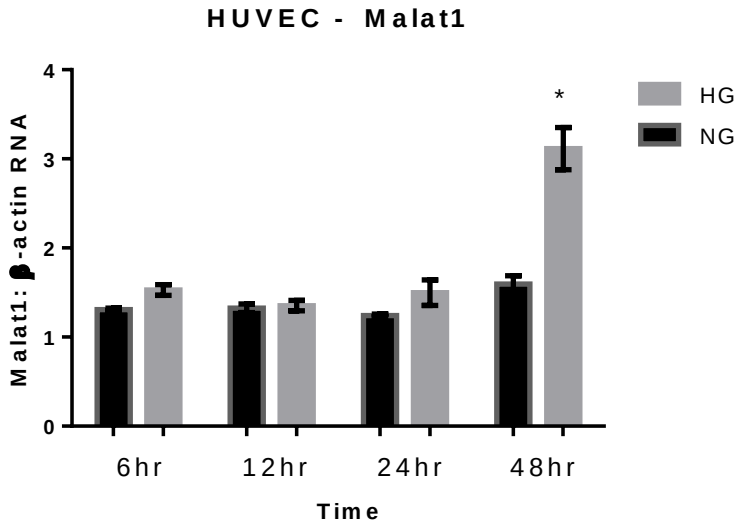

Figure 3.2: MALAT1 expression in HUVEC

Real time RT-PCR analysis of MALAT1 expression in HUVECs. Cells were exposed to 25 mM (HG) or 5 mM (NG) glucose over a time course of 48 hours. Levels of MALAT1 transcript were significantly increased in HG treated HUVEC at the 48 hour mark compared to the NG HUVEC. [* $p<0.05$ compared to NG, experiment performed in triplicate from three separate experiments, data (as a ratio to β-actin) expressed as mean ± SEM].

3.2 MALAT1 as a gene of interest

3.2.1 MALAT1 is a bona fide long non-coding RNA

Before taking our interest in MALAT1 to a higher organism, we first set out to investigate MALAT1 as a gene. Using bioinformatics software PhyloCSF we confirmed that MALAT1 is a non-coding RNA [Figure 3.3]. PhyloCSF uses amino acid arrangement and substitution frequencies in evolution to generate an odds likelihood ration upon whether the sequence is better explained as a coding sequence or a non-coding model. This is performed without the necessity of the sequence being similar to known proteins in current databases [101]. We compared it to known coding genes, as well as other non-coding genes. MALAT1 was identified as being 10^{11} times more likely to be explained by a non-coding than a coding model. No segment of MALAT1 was better explained by the coding model than the non-coding, and the greatest value was 10^{2} for a stretch of less than 35 nucleotides. Other non-coding genes were better explained by the non-coding model, and known coding genes were best explained by the coding model as was expected. This finding strongly suggests that MALAT1 is a non-coding transcript.

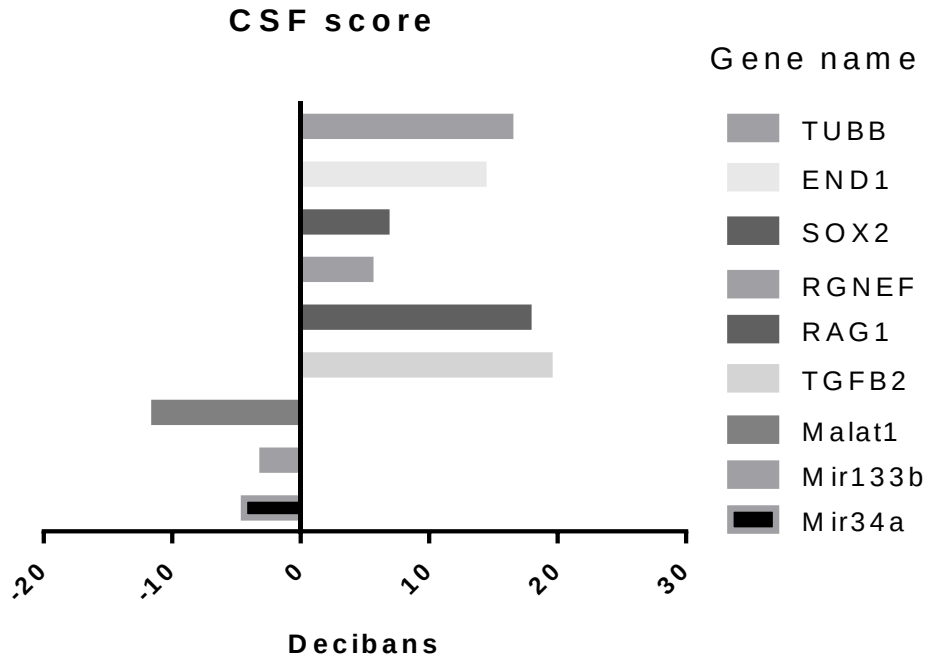

Figure 3.3: CSF scores

Codon Substitution Frequencies (CSF) scores of *TUBB*, *END1*, *SOX2*, *RGNEF*, *RAG1*, *TGFB2*, *Malat1*, *Mir133b*, and *Mir34a* RNA. PhyloCSF reports scores in decibans or log-ratio of whether a transcript is better explained by a coding or non-coding model. A score of 32 indicates a transcript is 10^{32} times more likely to be explained by the coding model than non-coding model, whereas a score of -11 would indicate a transcript is 10^{11} times more likely to be explained by the non-coding model than the coding model. PhyloCSF does not rely on homology of known coding sequences but rather evolutionary amino acid substitution as well as missense and nonsense substitution frequencies.

3.2.2 MALAT1 is present in the nucleus and is upregulated by glucose

Following confirmation of its lncRNA status, we looked at MALAT1 in HRECs using FISH to view the localization of MALAT1 in the cell. Using specific probes we located MALAT1 in the cells. Such analysis showed the presence and organization of MALAT1 in the nucleus. Our findings revealed that MALAT1 is an exclusively nuclear molecule and localizes to specific domains in the nucleus, which are known as paraspekles [Figure 3.4]. MALAT1's inability to leave the nucleus provides further evidence that it is not a coding gene.

We further used RT-PCR to look for differences in MALAT1 expression in HRECs to compare and validate our findings in HUVECs with a different cell type. As most of the diabetic complications under investigation are due to microvascular damage, capillary endothelial cells are of great interest in determining potential alterations of MALAT1 expression under high glucose conditions. RT-PCR expression of MALAT1 in HREC cells was consistent with our HUVEC experiment and showed a significant increase of MALAT1 in HREC cells at the 48hr time point when cells were treated with high glucose compared to control cells. Compared to normal glucose-treated cells, MALAT1 expression after 48hrs in the high glucose treatment was doubled. To examine potential downstream effects of MALAT1 upregulation, we examined several inflammatory cytokines. Under high glucose, these inflammatory cytokines are normally elevated compared to normal glucose conditions, and in diabetes this elevation leads to chronic levels of low grade inflammation. To this extent, we examined TNFα, IL6 and IL-1β. These are well established molecules that are upregulated in response to glucose in the context of chronic diabetic complications [103-105].We used qRT-PCR to quantify the expression of specific pro-inflammatory genes in the HREC cells.Expression of these genes increased in high glucose treatment compared to normal-glucose, and like MALAT1, this increase was significant in all tested genes at the 48-hour mark [Figure 4.5].

These findings taken together with literature on MALAT1 in other diseases and tissue expression made MALAT1 a promising candidate gene to look at in an *in vivo* model.

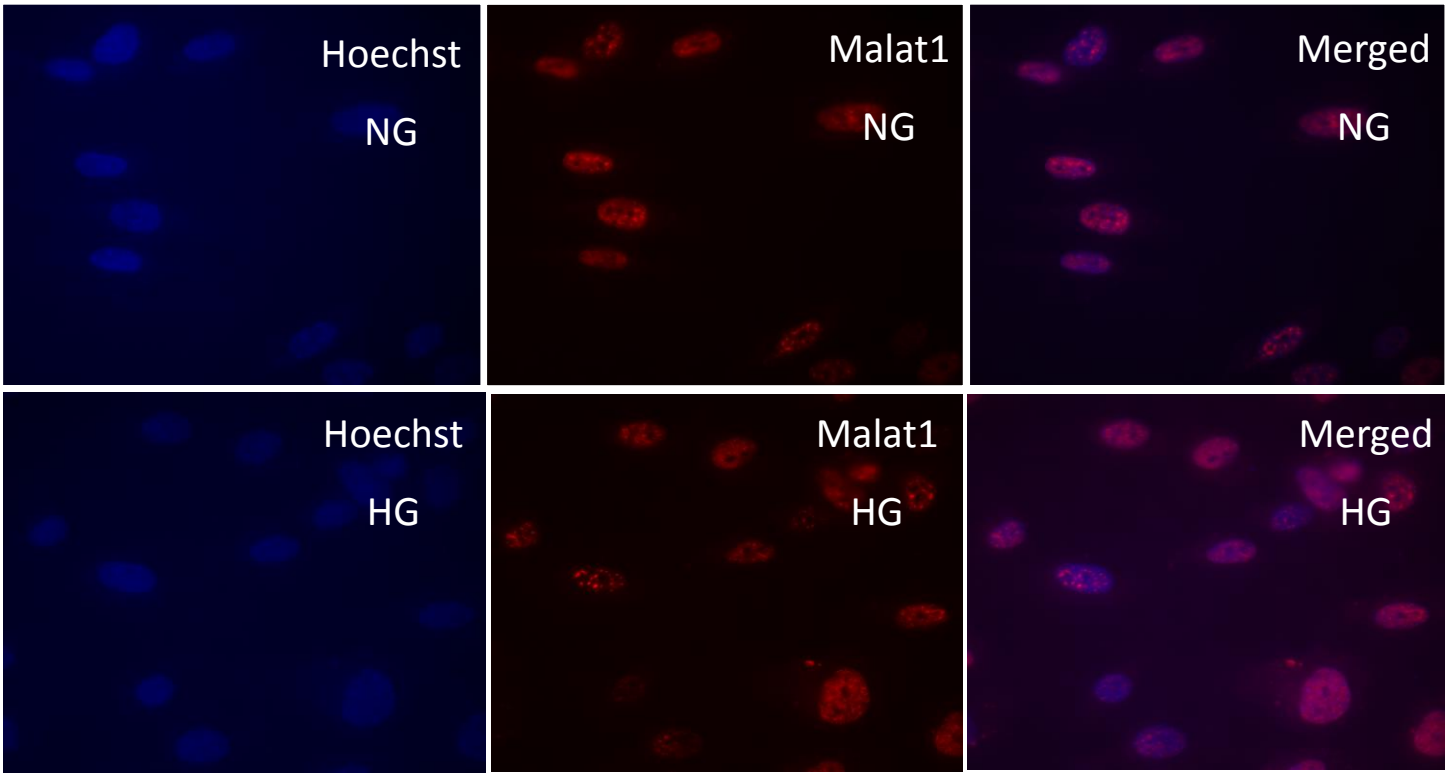

Figure 3.4: FISH visualization of MALAT1 lncRNA localization

MALAT1 is a completely nuclear retained lncRNA. Malat1 probes were used to detect presence of malat1 in HRECs using fluorescence. Cells that had been cultured in high glucose (25 mM) or normal glucose (5 mM) for 48 hours were hybridized with probes for MALAT1 RNA (red) then counterstained with Hoechst (Blue). Images were merged (purple) to show completely nuclear and speckled arrangement of MALAT1 lncRNA in the nuclei. No visual differences could be seen between HG and NG.

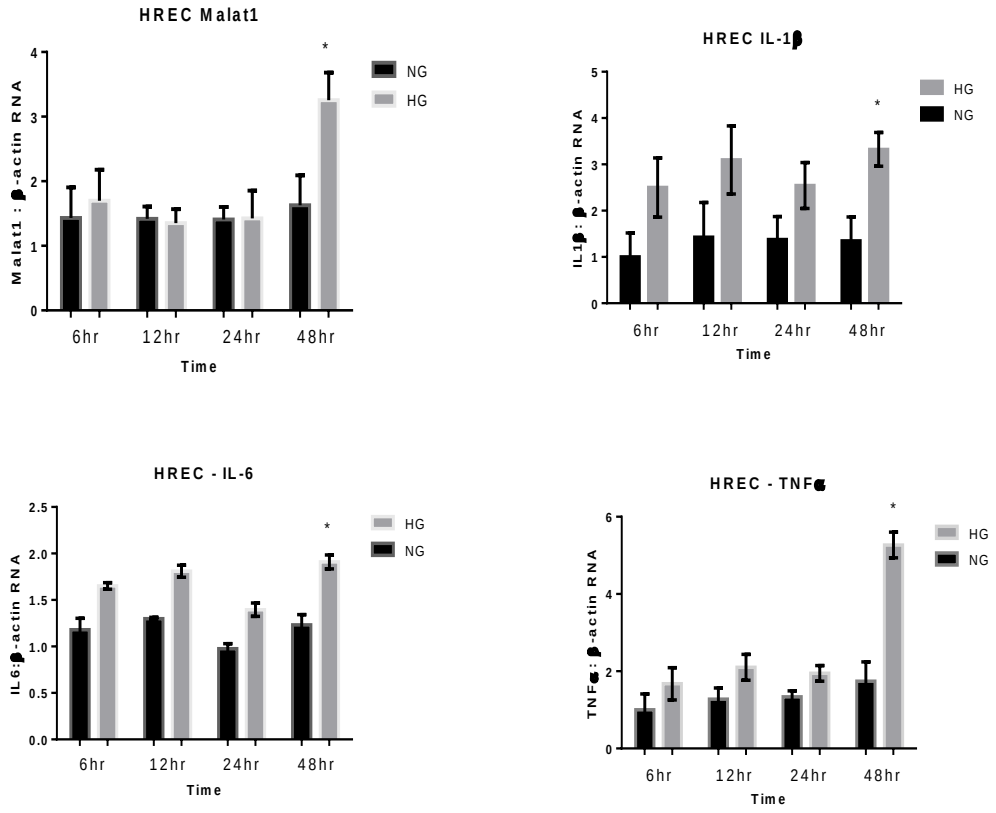

Figure 3.5: MALAT1 and inflammatory cytokine expression in HREC

Real time RT-PCR analysis of MALAT1, IL-1β, TNFα, and IL-6 expression in HRECs exposed to 25 mM (HG) or 5 mM (NG) glucose over a time course of 48 hours. All four genes are significantly upregulated in HG treated HRECs at 48 hours compared to NG. [* $p<0.05$ compared to NG, experiment performed in triplicate from three separate experiments, data (as a ratio to β-actin) expressed as mean ± SEM].

3.3 *In Vivo* Results

3.3.1 Clinical monitoring of Mice

MALAT1 knockout mice were generated by Dr. Spector using a C57/BL6 background [66]. Animals were obtained and the genetic background was confirmed using DNA genotyping [Figure 3.6]. Control mice on a C57/BL6 background were obtained from Charles River to be used as controls. Diabetes was confirmed in mice by measurement of blood glucose levels. Diabetic animals were hyperglycemic (>20.0 mmol/L glucose) and had reduced body weight gain compared to control animals [Figure 3.7]. Diabetic animals also showed polyuria, and glucosuria. None of the animals had measurable levels of ketones (data not shown). Loss of MALAT1 lncRNA had no effect on either the blood glucose level or the bodyweight gain and knockout animals showed no differences in urine output.

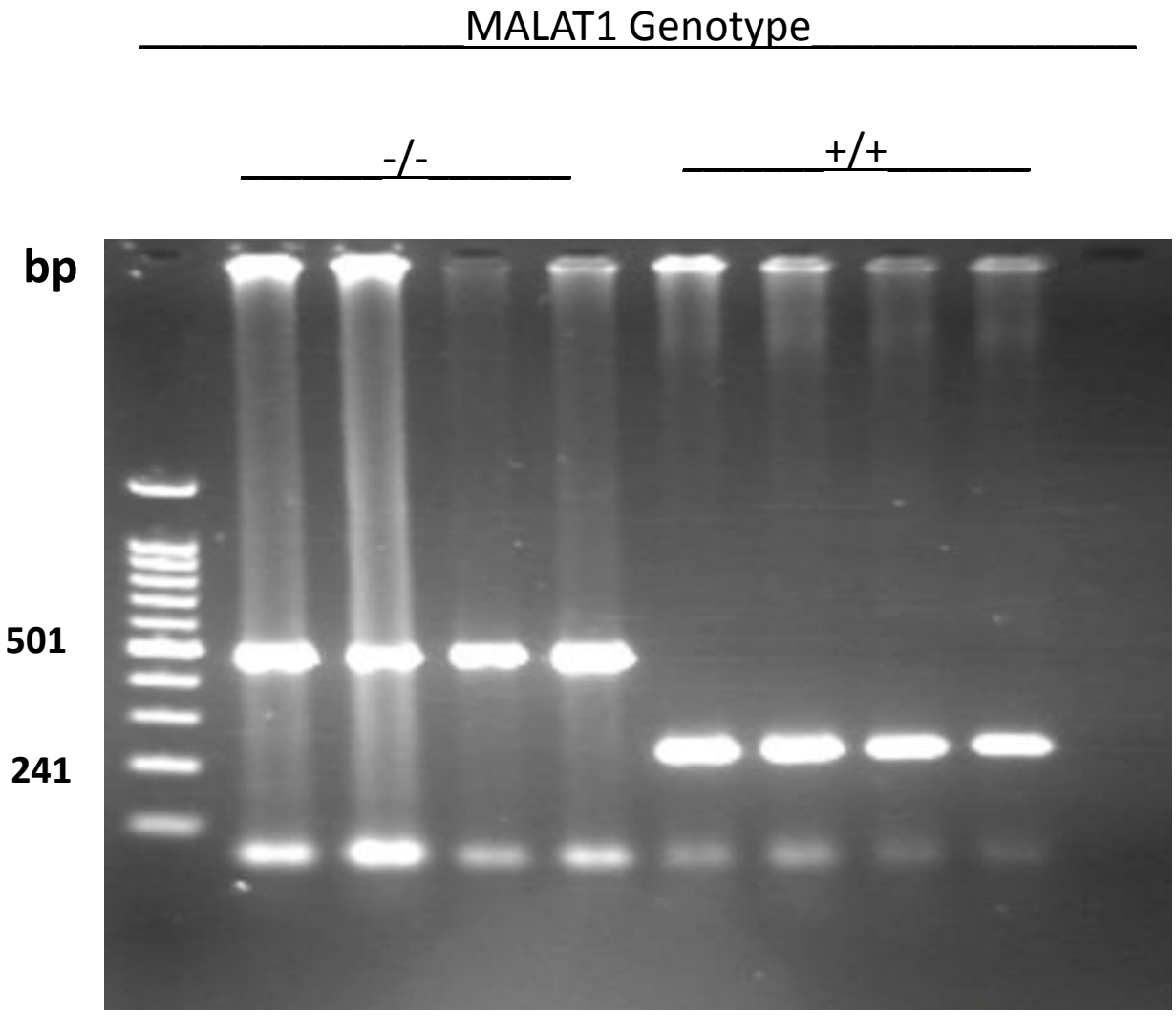

Figure 3.6: Genotype confirmation of MALAT1$^{-/-}$ mice

Analysis of MALAT1 genotype by PCR from tail DNA. Results indicate MALAT1 wild-type (+/+) and homozygous null (-/-) mice. DNA was resolved on a 1.5% agarose gel and imaged using UV light. A DNA ladder ranging from 100 to 1000 bp is shown in lane 1. Included base pair sizes denote predicted sizes for the KO and WT bands.

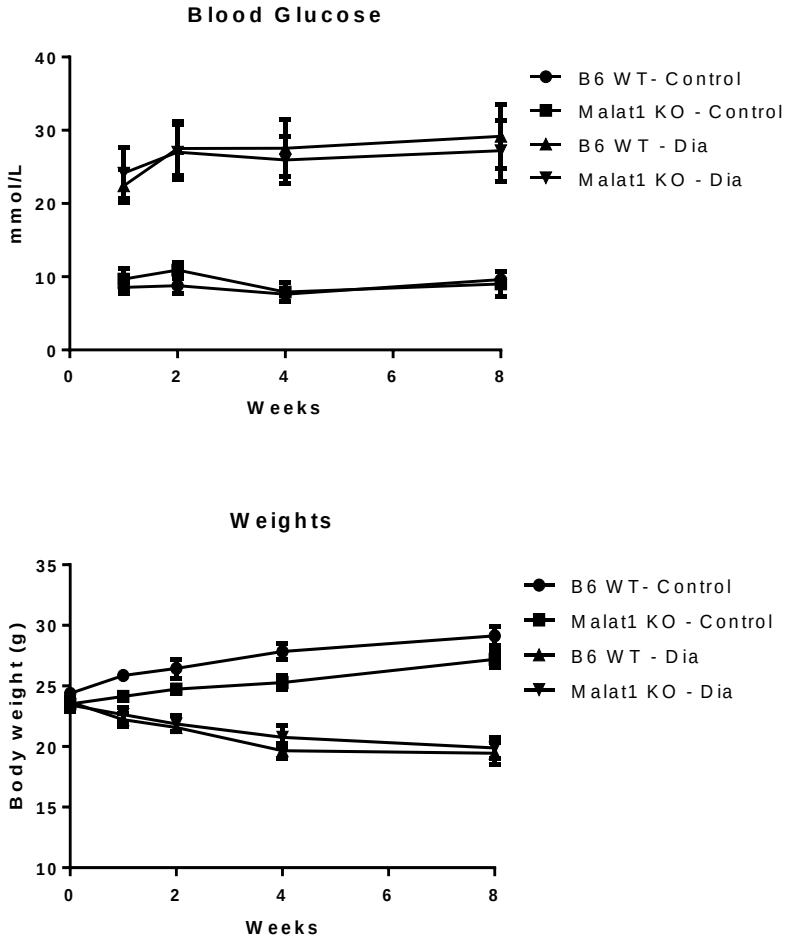

Figure 1.7: **Clinical monitoring**

Blood glucose values and body weights of mice during the follow up period. Mice were injected with STZ for five days following which they were checked for hyperglycemia (Time 0). Mice were examined regularly for 8 weeks. Both wild-type (WT) diabetic (Dia) animals, and MALAT1-/- (MALAT1 KO) animals were hyperglycemic compared to control animals at all time points and had reduced body weight gain. Loss of MALAT1 lncRNA had no significant effect on hyperglycemia or body weight gain in diabetes. [n=8-13; data expressed as mean ± SEM].

3.3.2 Diabetes alters MALAT1 expression in tissues

Using Real time PCR, MALAT1 transcript levels were measured in the heart, kidney and retina of WT control, WT diabetic, MALAT1 KO control, and MALAT1 KO diabetic animals. MALAT1 expression showed initial elevation in the kidneys from WT diabetic animals, followed by a decrease at 2, 4, and 8 weeks compared to the WT control tissue [Figure 3.8]. Both the kidney and heart tissue had significantly decreased levels of MALAT1 RNA in the WT diabetic animals compared to the WT control animals after two months of follow-up. [Figure 3.9]. There was no significant alteration in MALAT1 expression in B6 mouse retinal tissue at 2 months. MALAT1 KO animals were devoid of MALAT1 expression at all time-points in all tissues.

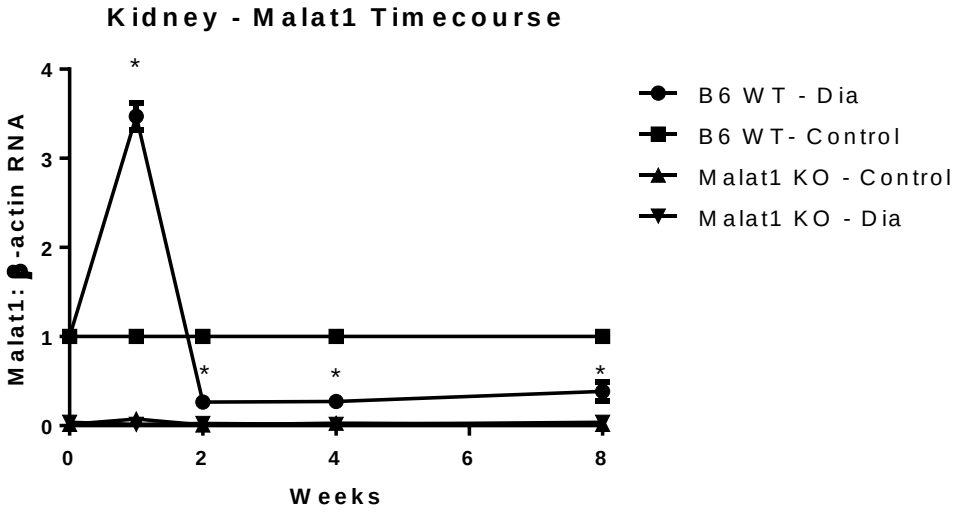

Figure 3.8: MALAT1 expression in diabetes over two months

Real time RT-PCR analysis of malat1in wild type (WT) control, WT diabetic (Dia), MALAT1$^{-/-}$ (MALAT1 KO) control, and MALAT1$^{-/-}$ diabetic mouse tissues. Transcript levels of MALAT1 RNA were significantly elevated in diabetic mouse kidney tissue at 1 week, following which it was reduced compared to the WT control mouse kidney tissue. [*$p<0.05$ compared to WT control; n=3-13; data (as a ratio to β-actin) expressed as mean ± SEM, normalized to controls].

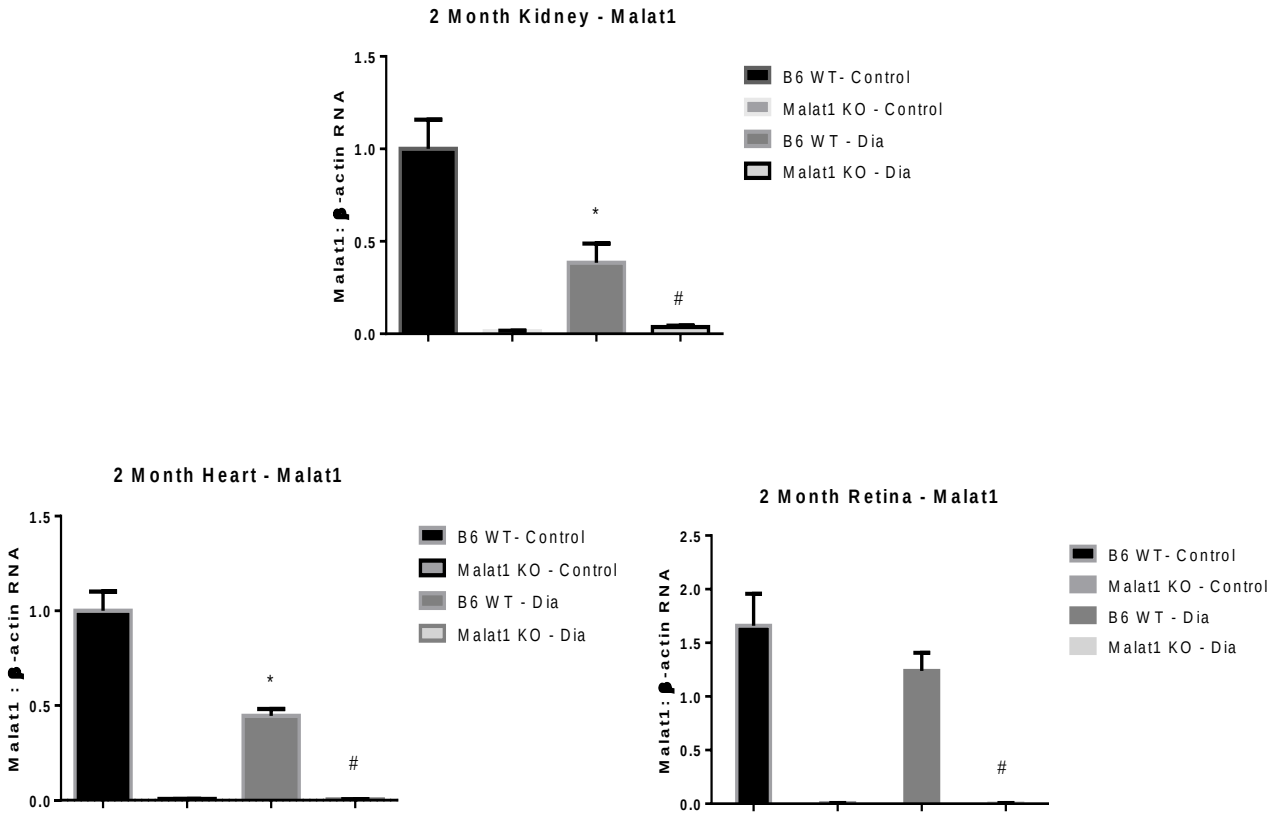

Figure 3.9: MALAT1 expression in heart, kidney, and retina at 2-months

Real time RT-PCR analysis of malat1 in wild type (WT) control, WT diabetic (Dia), MALAT1$^{-/-}$ (MALAT1 KO) control, and MALAT1$^{-/-}$ 2-month diabetic mouse kidney, heart and retinal tissue. Transcript levels of MALAT1 were significantly decreased in diabetic mouse heart and kidney tissue compared to the WT controls. MALAT1 RNA was not present in any of the knockout tissues. MALAT1 expression was not significantly altered in the retinal tissue. [*$p<0.05$ compared to WT control; n=6-13; data (as a ratio to β-actin) expressed as mean ± SEM].

3.3.3 MALAT1 regulates inflammatory cytokine expression the tissues of chronically diabetic animals.

Having both confirmed that MALAT1 lncRNA levels are altered in diabetes in our *in vivo* model, as well as having confirmed our MALAT1 KO model, we tested for transcripts with changes in expression that might be attributed to the loss of MALAT1 RNA in diabetes. We focused on kidney and heart tissues first due to the availability of tissue.

Using RT-PCR, we measured the inflammatory cytokine transcript levels of IL-1β, IL-6 and TNFα in both 1 and 2-month heart and kidney tissue. IL-1β and TNFα transcript abundances were upregulated in the WT diabetic animals compared to WT controls in both heart and kidney at both time points [Figures 3.10, 3.11, 3.12, and 3.13]. IL-6 was upregulated in both heart and kidney tissues at the 1-month time point, and kidney tissue at the 2-month time point in WT diabetics compared to WT controls. Loss of MALAT1 prevented diabetes induced increase of inflammatory transcripts in both heart and kidneys after both one and two months of diabetes.

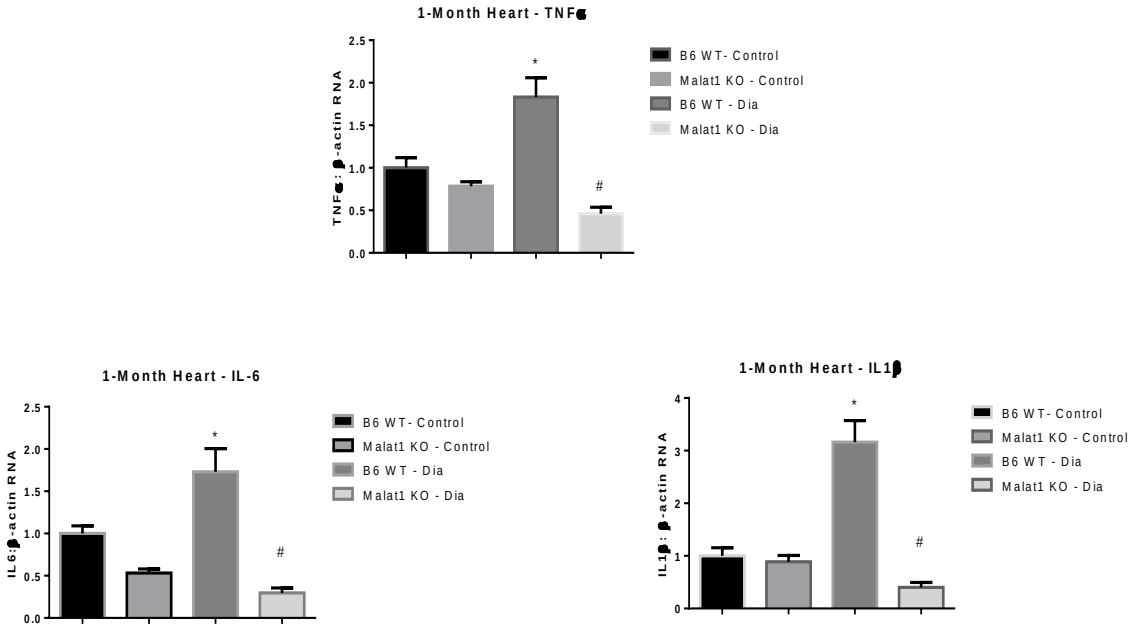

Figure 3.10: Inflammatory transcript expression at 1-month diabetes in heart tissue

Real time RT-PCR analysis of TNFα, IL-6, and IL-1β in wild type (WT) control, WT diabetic (Dia), MALAT1$^{-/-}$ (MALAT1 KO) control, and MALAT1$^{-/-}$ 1-month diabetic mouse cardiac tissues. All three transcripts were significantly increased in diabetic mouse heart tissue compared to the WT controls. Loss of MALAT1 RNA prevented such increases in the MALAT1 KO diabetic group. [*$p<0.05$ compared to WT control; #$p<0.05$ compared to WT Dia; n=8-13; data (as a ratio to β-actin) expressed as mean ± SEM, normalized to controls].

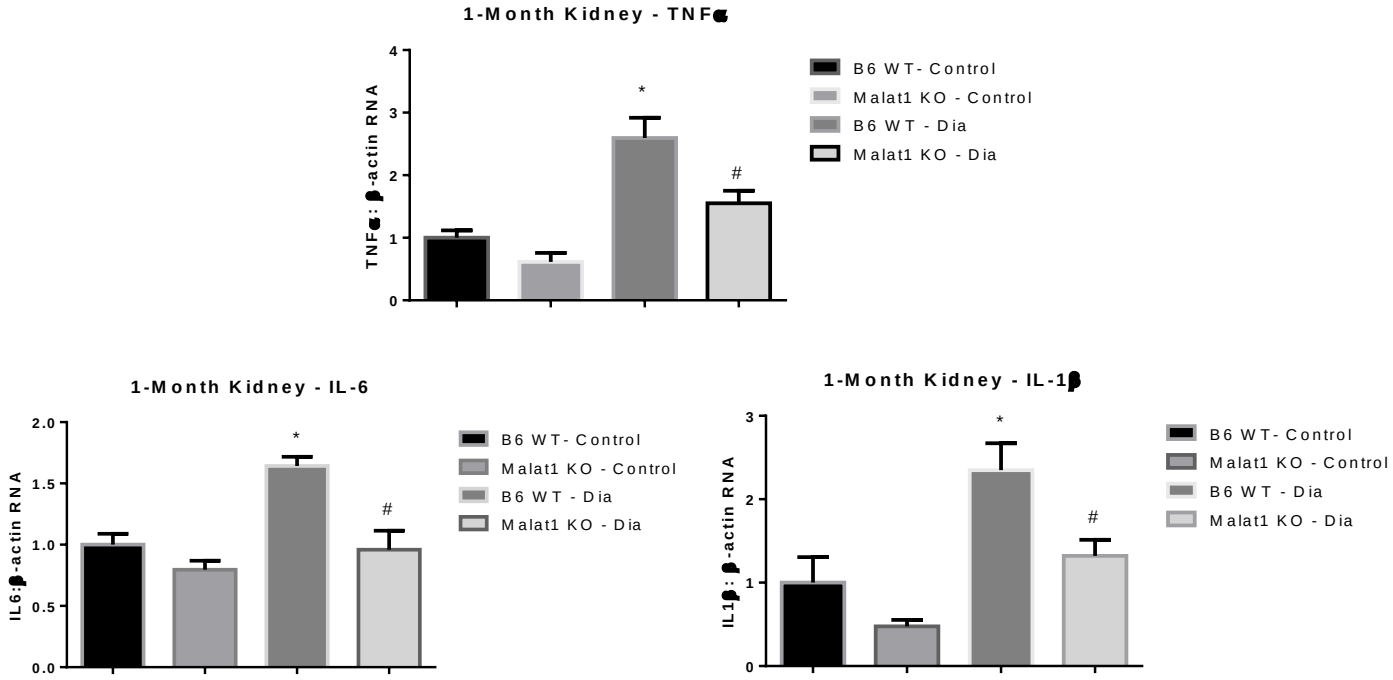

Figure 3.11: Inflammatory transcript expression at 1-month diabetes in kidney tissue

Real time RT-PCR analysis of TNFα, IL-6, and IL-1β in wild type (WT) control, WT diabetic (Dia), MALAT1$^{-/-}$ (MALAT1 KO) control, and MALAT1$^{-/-}$ 1-month diabetic mouse renal tissue. All three genes were significantly increased in diabetic mouse kidney tissue compared to the WT controls. Loss of MALAT1 lncRNA prevented such increases in the MALAT1 KO diabetic group. [*$p<0.05$ compared to WT control; #$p<0.05$ compared to WT Dia; n=6-10; data (as a ratio to β-actin) expressed as mean ± SEM, normalized to controls].

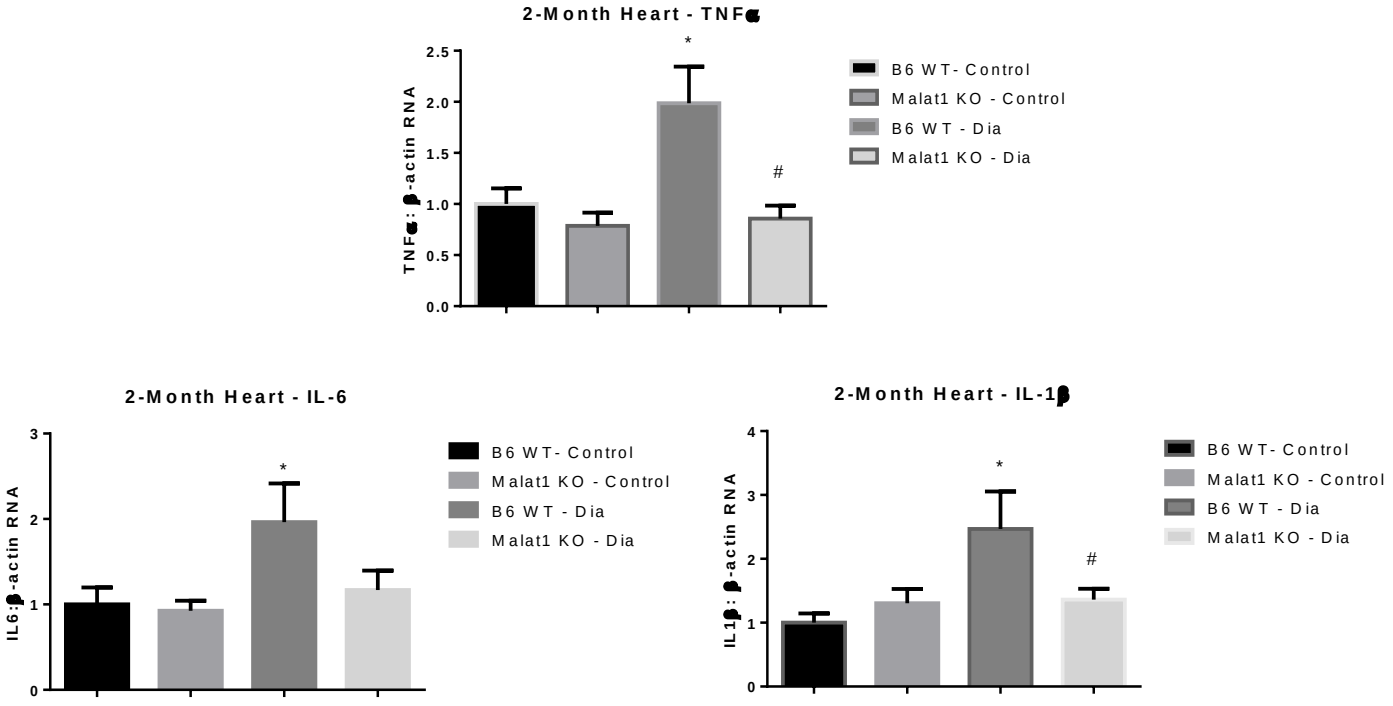

Figure 3.12: Inflammatory transcript expression at 2-month diabetes in heart tissue

Real time RT-PCR analysis of TNFα, IL-6, and IL-1β in wild type (WT) control, WT diabetic (Dia), MALAT1$^{-/-}$ (MALAT1 KO) control, and MALAT1$^{-/-}$ 2-month diabetic mouse cardiac tissue. All three genes were significantly increased in diabetic mouse heart tissue compared to the WT controls. Loss of MALAT1 lncRNA prevented such increases in the MALAT1 KO diabetic group for both IL-1β and TNFα but not for IL-6. . [*$p<0.05$ compared to WT control; #$p<0.05$ compared to WT Dia; n=8-13; data (as a ratio to β-actin) expressed as mean ± SEM, normalized to controls].

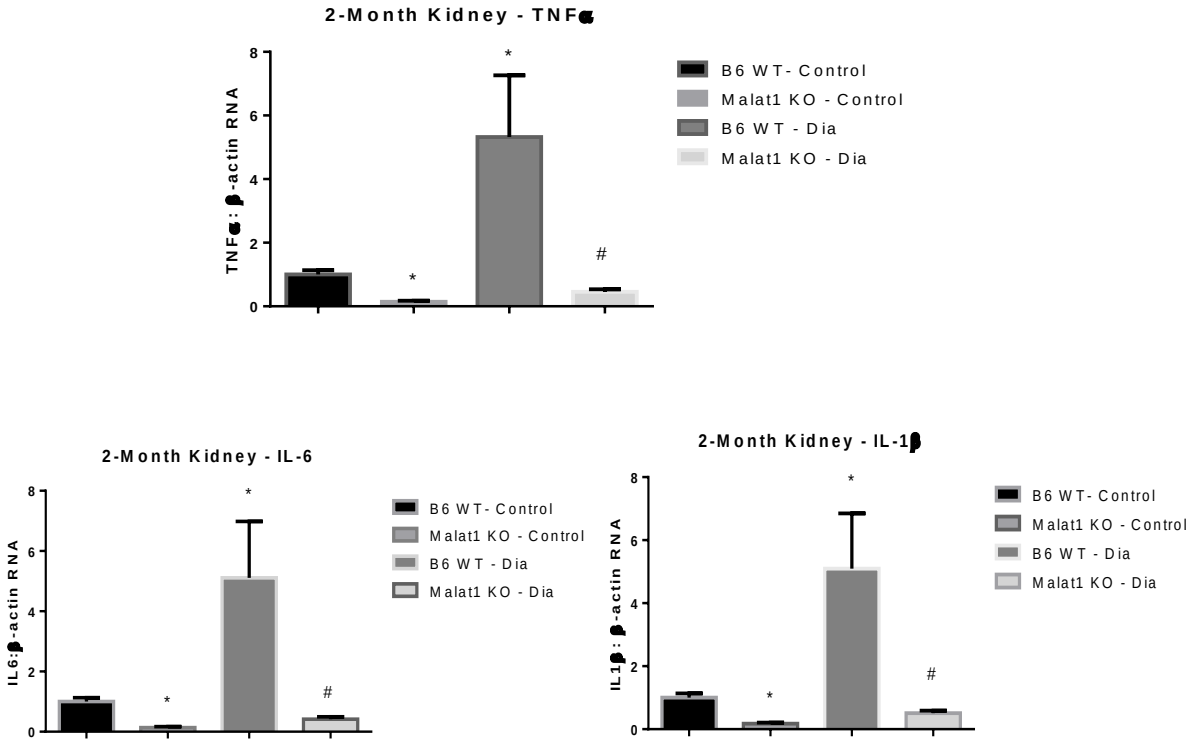

Figure 3.13: Inflammatory transcript expression at 2-month diabetes in kidney tissue

Real time RT-PCR analysis of TNFα, IL-6, and IL-1β in wild type (WT) control, WT diabetic (Dia), MALAT1$^{-/-}$ (MALAT1 KO) control, and MALAT1$^{-/-}$ 2-month diabetic mouse renal tissue. All three transcripts were significantly increased in diabetic mouse kidney tissue compared to the WT controls. Loss of MALAT1 lncRNA prevented such increases in the MALAT1 KO diabetic group. MAlAT1 KO control mice had significantly less expression of all three genes than the WT control mice. [*$p<0.05$ compared to WT control; #$p<0.05$ compared to WT Dia; n=4-9; data (as a ratio to β-actin) expressed as mean ± SEM, normalized to controls].

3.3.4 Protein expression

This finding was then further confirmed using protein extract from kidney and heart. We used ELISAs to test for levels of the pro-inflammatory cytokines IL-6 and INFγ in tissue lysates from both heart and kidney and IL-1β in kidney. Our findings corroborated those of our transcript analyses and showed significant elevation in inflammatory cytokine production in WT diabetic animals, and protection from this increase in the MALAT1 knockout diabetic animals for each of the cytokines tested in both tissues [Figures 3.14 and 3.15].

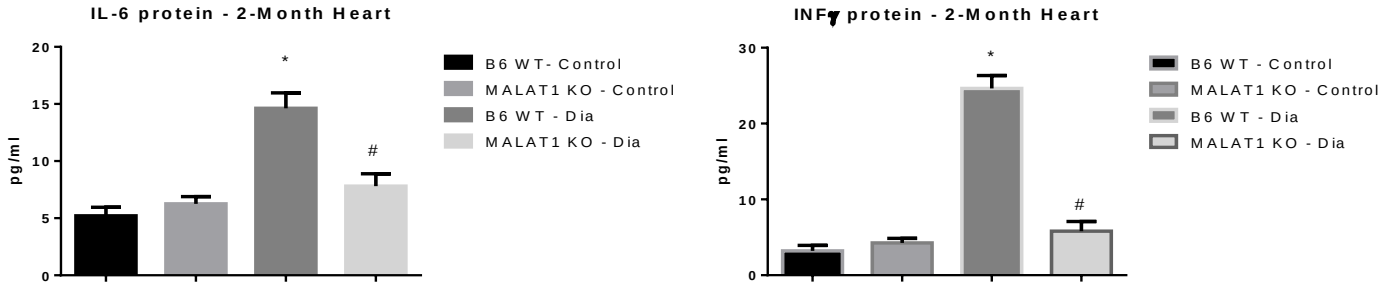

Figure 3.14: Inflammatory cytokine expression in 2-month heart tissue

ELISA for mouse IL-6 and INFγ in wild type (WT) control, WT diabetic (Dia), MALAT1$^{-/-}$ (MALAT1 KO) control, and MALAT1$^{-/-}$diabetic 2-month cardiac tissue. Both cytokines were significantly increased in diabetic mouse heart tissue compared to the WT controls. Loss of MALAT1 lncRNA prevented such increases in the MALAT1 KO diabetic group. MALAT1 KO control mice had comparable expression to WT control mice. [*$p<0.05$ compared to WT control; #$p<0.05$ compared to WT Dia; n=5-9; data expressed as mean ± SEM].

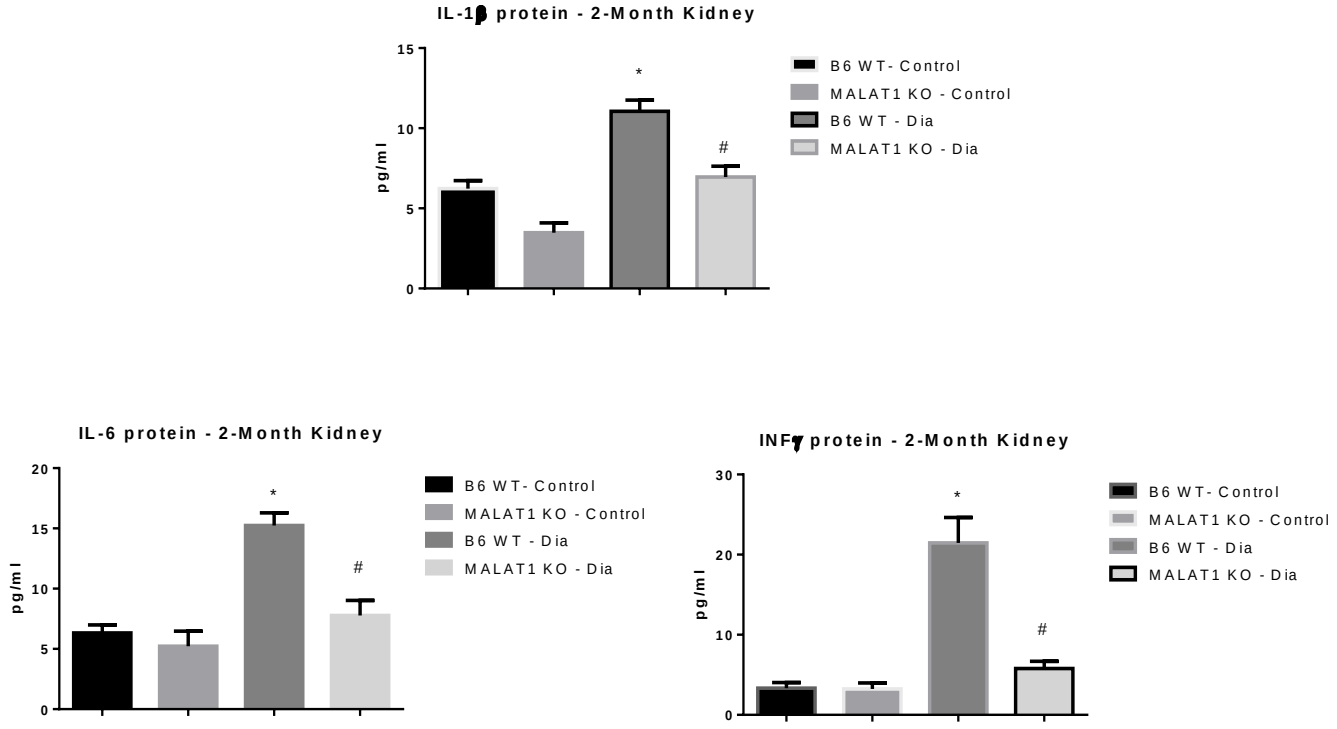

Figure 3.15: Inflammatory cytokine expression in 2-month kidney tissue

ELISAs for mouse IL-6, IL-1β, and INFγ in wild type (WT) control, WT diabetic (Dia), MALAT1$^{-/-}$ (MALAT1 KO) control, and MALAT1$^{-/-}$ diabetic 2-month renal tissue. All three cytokines were significantly increased in diabetic mouse kidney tissue compared to the WT controls. Loss of MALAT1 lncRNA prevented such increases in the MALAT1 KO diabetic group. MALAT1 KO control mice had comparable expression to WT control mice. [*$p<0.05$ compared to WT control; #$p<0.05$ compared to WT Dia; n=5-9; data expressed as mean ± SEM].

3.3.5 Potential interactions of MALAT1

We looked at multiple genes of interest that may be involved in MALAT1 regulation or downstream of MALAT1. Three candidate genes were SAA3, NEAT1, and p53. SAA3, a regulator of inflammation, has previously been shown to be diminished in MALAT1 KO mice [66]. Our study supports this finding, as well as provides new evidence for MALAT1's regulation of SAA3 using diabetic animals. SAA3 was found to be significantly elevated in the WT diabetic animals, but loss of MALAT1 lncRNA prevented this increase in both heart and kidney [Figures 3.16, 3.17]. We further examined two other potential molecules regulated by MALAT1 as proposed by literature, these being NEAT1 and p53. NEAT1 is the neighboring gene of MALAT1 and is also an evolutionary conserved lncRNA [83]. Neat1 was also shown to be elevated in the liver and brain cortex of MALAT1 knockout mice compared to WT animals in a previous study [66]. While diabetes had no significant effect on neat1, we confirmed that loss of MALAT1 led to significant increases in the transcript compared to WT animals in both the heart and kidney tissues [Figures 3.14, and 3.15]. P53 has been investigated as both an upstream as well as a downstream mediator of MALAT1 [89.92,93]. At 2-months post diabetes in the heart tissue, p53 transcript was significantly elevated compared to WT control animals, and this increase was attenuated in the MALAT1 KO diabetic animals [Figure 3.14]. However, in the kidney tissue, both MALAT1 KO groups and the diabetic WT animals had significantly elevated levels of p53, suggesting a tissue specific altered regulation [Figure 3.17].

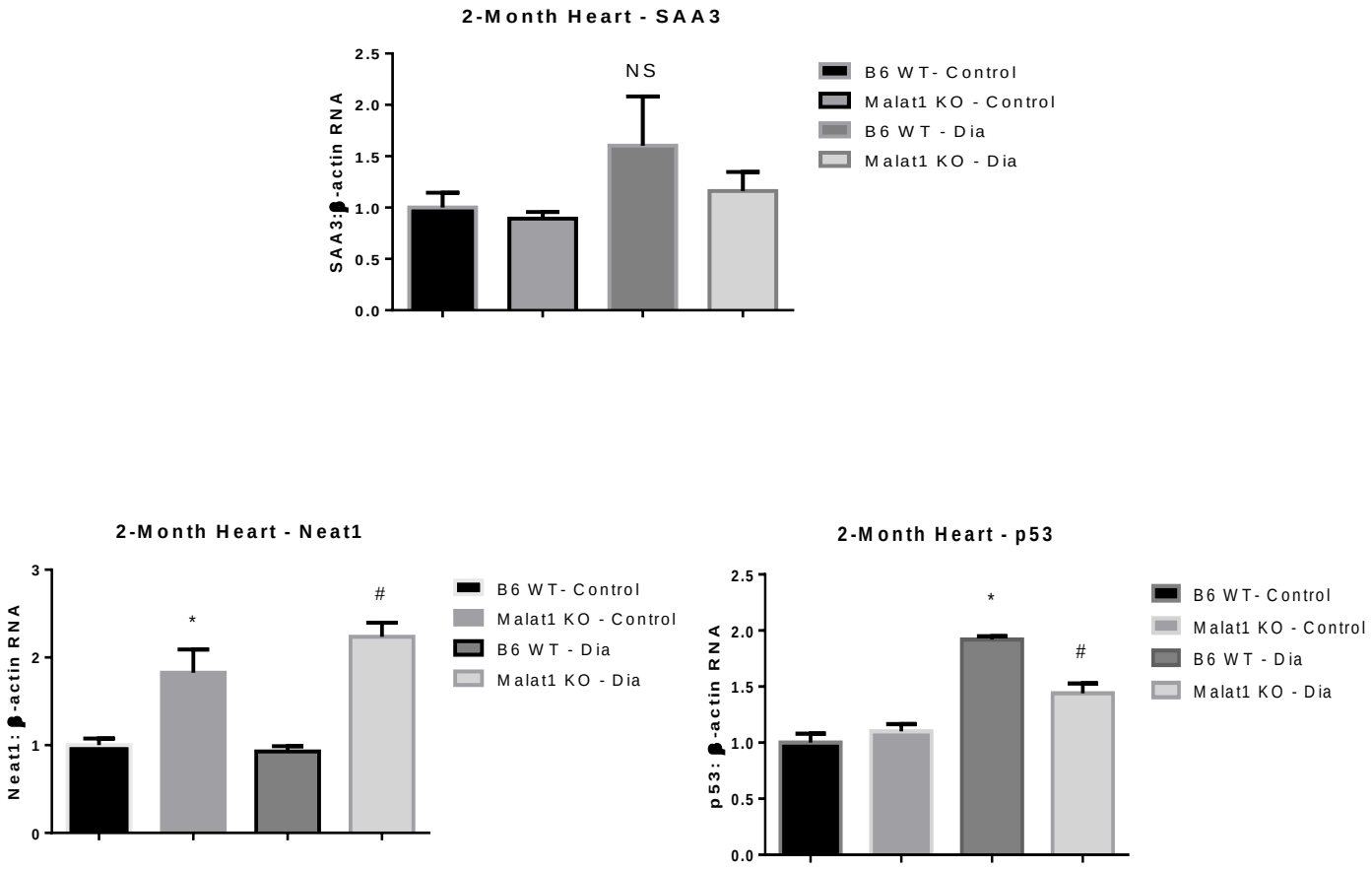

Figure 3.16: Molecular alterations downstream to malat1 knockout in 2-month heart tissue

Real time RT-PCR analysis of SAA3, p53, and neat1in wild type (WT) control, WT diabetic (Dia), MALAT1$^{-/-}$ (MALAT1 KO) control, and MALAT1$^{-/-}$ 2-month diabetic mouse cardiac tissues. SAA3 was not found to be significantly altered in diabetes. Relative abundance of p53 was significantly increased in the WT diabetic animals. Loss of MALAT1 lncRNA prevented such increases in the MALAT1 KO diabetic group. Neat1 transcript abundance was significantly increased in both MALAT1 KO groups. [*$p<0.05$ compared to WT control; #$p<0.05$ compared to WT Dia; n=6-10; data expressed (as a ratio to β-actin) as mean ± SEM, normalized to controls].

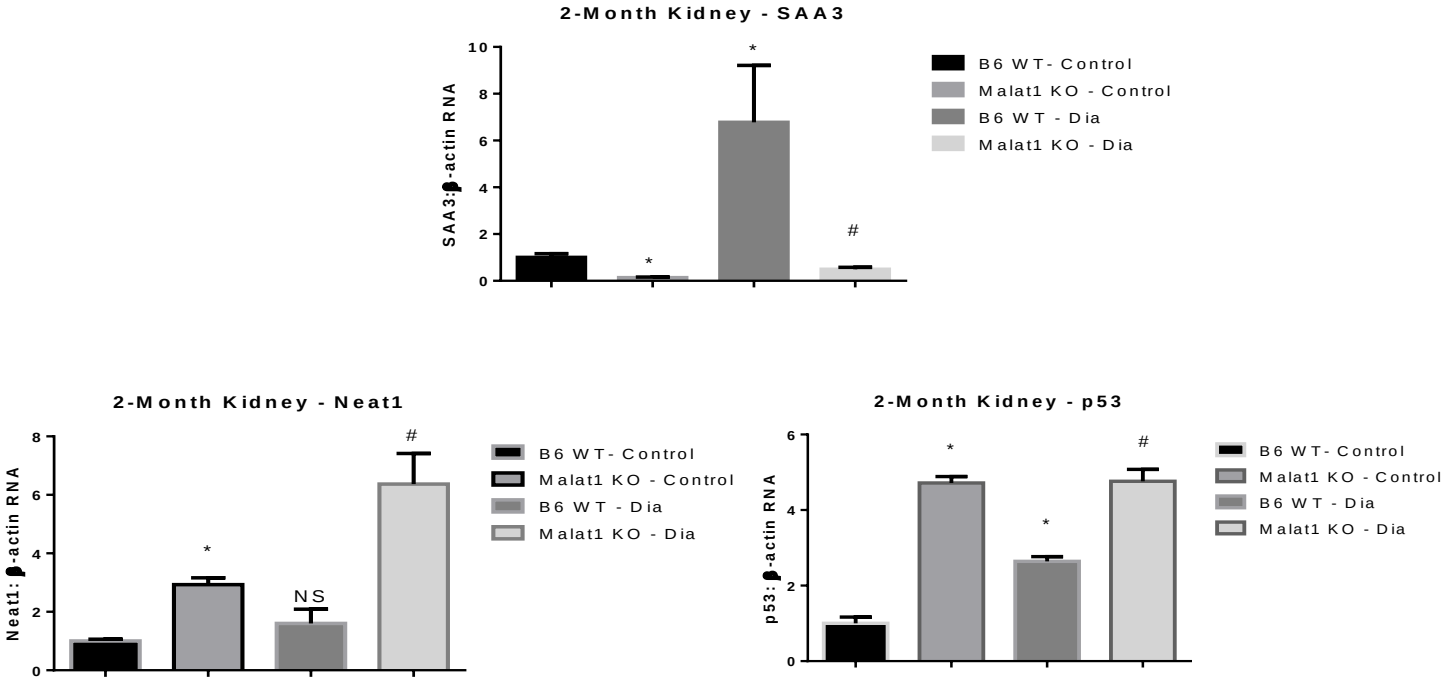

Figure 3.17: Molecular alterations downstream to MALAT1 lncRNA knockout in 2-month kidney tissue

Real time RT-PCR analysis of SAA3, p53 and Neat1 in wild type (WT) control, WT diabetic (Dia), MALAT1$^{-/-}$ (MALAT1 KO) control, and Malat1$^{-/-}$ diabetic 2-month diabetic mouse renal tissue. SAA3 was significantly increased in diabetic mouse kidney tissue compared to the WT controls. Loss of malat1 prevented such increases in the MALAT1 KO diabetic group. P53 was significantly increased in the WT diabetic mice as well as both MALAT1 KO groups compared to the WT controls. Transcript abundance of neat1 was significantly increased in both the MALAT1 KO groups compared to the WT control mice. [*$p<0.05$ compared to WT control; #$p<0.05$ compared to WT Dia; n=4-9; data (as a ratio to β-actin) expressed as mean ± SEM, normalized to controls].

3.4 Functional Analyses

Renal and cardiac functional analyses were performed for both the kidneys and the heart to assess the effect of diabetes on target organ damage and whether such changes are specifically mediated through MALAT1 and other biochemical alterations.

3.4.1 Albumin Creatinine Ratio (ACr ratio)

ACr ratio was used to assess kidney function over the course of one day. This is a standard test for assessing kidney function [106,107]. Albumin is a large protein that is normally only present in the urine in very small quantities due to its large size being unable to pass through the glomeruli. In diabetes however, damage to the kidney by glucose-induced alterations leads to widening in pore sizes, which allows larger proteins to pass through and further damage the kidney. As such, albuminuria is one of the earliest and most characteristic functional changes in diabetic nephropathy [108]. Creatinine on the other hand is a protein compound that is released regularly over the course of a day as a by-product of normal muscle breakdown [109]. Lower as well as higher than normal creatinine levels have both been associated with diabetes; however, in most cases the levels do not appear to be altered in diabetes due to similar skeletal muscle abundances in diabetic and non-diabetic animals [110,111]. Briefly, two days before sacrifice, urine was collected for 24 hours and the total volume was recorded. Urine samples were kept and frozen in -80 °C to be used in future analyses. ELISAs were used independently to measure the amount of albumin and creatinine in the urine samples, the ratios were obtained, and were normalized to 24 hr urine volume. The WT diabetic as well as the MALAT1 KO diabetic animals showed significantly increased ACr ratio compared to the WT control animals [Figure 3.18]. Loss of MALAT1 lncRNA had no effect on the ACr ratio in MALAT1 KO control animals.

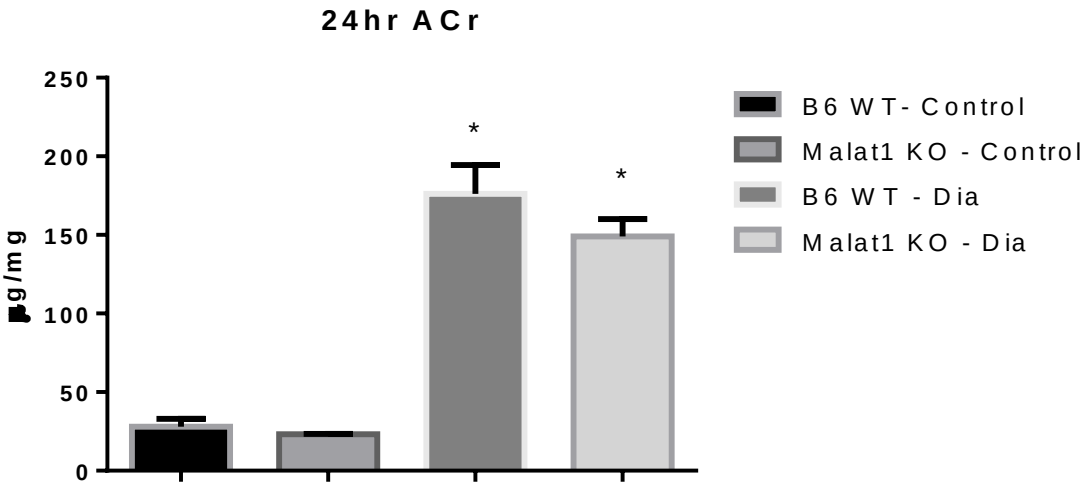

Figure 3.18: Mouse 24 hr albumin: creatinine ratio in 2-month diabetic mice

Urinary albumin/creatinine ratio measured in in wild type (WT) control, WT diabetic (Dia), MALAT1$^{-/-}$ (MALAT1 KO) control, and MALAT1$^{-/-}$ diabetic mice following 2 months of STZ-induced diabetes. Diabetic animals had significantly higher albumin/creatinine ratios compared to the control animals. MALAT1 had no significant effect in reducing the diabetes-associated increase. [*$p<0.05$ compared to WT control; n=8-10; data expressed as mean ± SEM].

3.4.2 Doppler Echocardiography

In the heart, echocardiography was used to look at and measure blood flow in the left ventricle, as well as heart wall thickness. We used the VEVO2100 ultrasound to carry out this procedure 5 days prior to sacrifice. In diabetes, the heart loses some of its contractility due to changes in the cardiomyocytes. This causes normal blood flow patterns to be altered which can be measured using pulsewave Doppler [112]. The E/A wave ratio is one metric used to look at the amount of blood that moves through the mitral valve during normal filling of the left ventricle. In normal hearts, the majority of the blood moves in to the ventricle during the E (early) wave and a smaller remaining amount is pushed into the heart by arterial contraction in the A (late) wave. However, in diabetes, only about half the blood moves into the heart in the diastolic filling or E wave, and much more blood has to be pushed through during the A wave leading to a lower E/A ratio. Both MALAT1 control and WT control animals showed normal E/A ratios [Figure 3.19]. WT diabetic animals had significantly decreased E/A ratios, indicating some diastolic dysfunction. Loss of MALAT1 in diabetic animals had partial protective effect on diabetes induced dysfunction. Supplemental data can be found in Table 3.1.

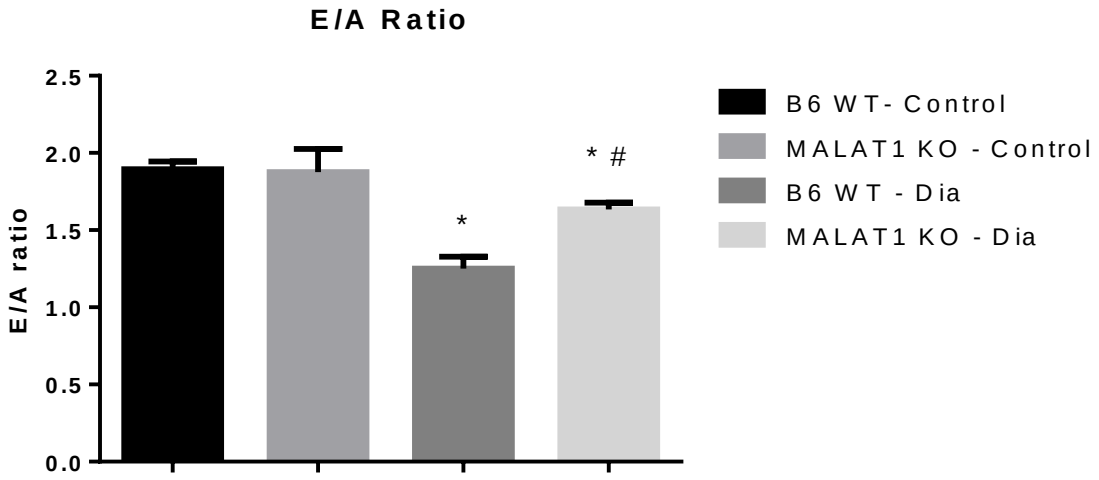

Figure 3.19: Loss of MALAT1 prevents functional alterations in heart contractility in diabetes

Using a Vevo2100 ultrasound we conducted echocardiographic examinations to assess functional changes in heart contractility of MALAT1$^{-/-}$ (MALAT1 KO)control, WT diabetic (Dia) and MALAT1$^{-/-}$ diabetic mice compared to wild-type (WT) control mice. 2-month WT diabetic mice showed reduced E/A ratio compared to WT control animals. Such changes were partially corrected in the MALAT1 knockout diabetic animals. MALAT1 knockout control animals showed no differences in E/A ratio compared to WT control animals. [*p<0.05 compared to WT control; #p<0.05 compared to WT Dia; compared to WT control; n=8-12; data expressed as mean ± SEM].

Table 3.1: Echocardiographic data

Variable	WT-Co (n=6)	MALAT1-Co (n=6)	WT-Dia (n=6)	MALAT1-Dia (n=6)
Diastolic Function				
E'/A' ratio	1.585±0.155	1.675±0.141	1.29±0.103	1.410±0.132
Haemodynamics				
Heart rate (beats/min)	401±16	391±35.57	430±40.40	410±31.12

Note: WT-Co, wild type control; WT-Dia, wild type diabetes; MALAT1-Co; MALAT1 knockout control, MALAT1-Dia; MALAT1 knockout with diabetes.

Chapter 4

4 Discussion

This study looked at the role of MALAT1 in producing inflammatory cytokines in chronic diabetic complications. Here we have examined a novel mechanism that takes place in diabetes to regulate the production of inflammatory cytokines using a long non-coding RNA. Furthermore, this is the first study to look at MALAT1 in a chronic diabetic animal model. This study expands on the current knowledge of diabetic complications and immune transcript regulation in the nucleus, and provides novel insight and findings in the field of lncRNA.

Inflammation is a key process in the development of diabetic complications [13,14]. High glucose in the blood initially leads to the impairment of glycolytic metabolism and an increase in reactive oxygen species in the cells. Oxidative DNA can then act as a danger-associated signal which can be recognized by internal receptors which trigger the production of these inflammatory molecules [34,35]. Low-grade chronic inflammation is continuously present in sites that are affected by the disease. This leads to a pro-inflammatory environment and recruitment of larger than normal numbers of inflammatory cells which mediate many of the pathologies associated with diabetic complications [13,14]. These conditions lead to continual damage to the inflamed tissues due to the secreted molecules and actions taken by the immune cells. Inflammation is also a key process involved in cancer metastasis where levels of MALAT1 RNA are greatly elevated. MALAT1 was also previously shown to be involved in the regulation of inflammatory cytokines in other systems [66,95].

We identified MALAT1 as one of many lncRNAs that was upregulated in endothelial cells when exposed to high glucose using an array. Using a local alignment tool, probe sequences were compared across the human genome and one was identified as a complete 60-nucleotide match identical to human MALAT1. In this case, MALAT1 lncRNA was downregulated almost 3-fold in the human retinal endothelial cells

compared to the control treated cells.

However, when we examined cells using RT-PCR to validate the array findings we were surprised to see a duration dependent alteration of glucose induced MALAT1 expression. Although in keeping with array study, it was downregulated after 24hrs, following 48hrs of high glucose, it was increased. We confirmed these findings in two endothelial cells and then explored further effects of such upregulation. The exact reason for such variability is not clear. Several explanations may be put forward. The sensitivity of the assay (array vs. RT-PCR), and RNA degradation may both be in part responsible. In addition, other factors induced secondary to oxidative stress may also be responsible. Nevertheless, the biological significance of such alterations were demonstrated following siRNA mediated silencing [95].

MALAT1 is one of the more characterized lncRNAs although it still remains largely unstudied due to its relatively recent discovery in 2003 [75]. Several papers have proposed functions or mechanisms for the molecule, but there is little consensus and novel findings continue to be reported. A likely reason for this may be due to tissue specific or cell-specific functions. MALAT1is expressed at high levels in nearly all cell types but it is quite possible that it does not exert the exact same function in each cell [89]. MALAT1 lncRNA is an extremely large molecule at 8.7 kb in humans, so it is even more likely that the molecule has multiple functions in a given cells rather than just one. MALAT1 is highly conserved evolutionarily [92], so it is possible that MALAT1 may have evolved to have a specific function that only presents itself under a particular stress.

MALAT1 has been shown to be a true lncRNA [84]. It was shown recently that about five percent of proposed lncRNAs actually coded for small peptide sequences [103]. Several others are still debated due to their homology to protein coding transcripts or strong association with ribosomes. MALAT1 has been shown to be a long noncoding RNA through multiple means including bioinformatics analyses, localization, ribosomal affinity, and *in vitro* transcription-translation assays [78, 66]. Such assays use both biotechnological and quantitative experiments to look at the affinity of the transcript for

ribosomes, and the presence of specifically sized bands matching open reading frame (ORF) sizes in Western blots. We have also confirmed this ourselves using the bioinformatics software PhyloCSF which found MALAT1 RNA to be 10^{11} times to be better explained by a non-coding transcript model than a coding model. This software is also highly used and recognized due to its coding which allows it to not only consider known protein sequences but account for the possibility of uncharacterized or unknown sequence arrangements [101,102].

Here we further show MALAT1 lncRNA is an exclusively nuclear lncRNA which again supports its classification as a lncRNA. This finding has been shown by other labs previously [66,86]. We do, however show that MALAT1 lncRNA localization in the nucleus does not appear to change under high glucose treatment. Using florescent probes specific to MALAT1 RNA we were able to show that (lncRNA) MALAT1 retains its focal expression pattern under both high and low glucose treatments in endothelial cells. No visual differences could be seen between HG and NG using this method, which is why RT-PCR analysis was conducted to show changes in MALAT1 expression more sensitively.

We looked at MALAT1 expression levels and we compared levels of transcripts of interest using qRT-PCR in the high and low glucose treated cells. We first found that at 48-hours, MALAT1 was upregulated more than two fold in the high glucose treated cells compared to normal glucose treated cells. However, MALAT1 expression was not significantly different between the treated cells and controls at 6, 12, or 24 hours. This same pattern was identified in both HREC and HUVEC cells.

Many transcripts have altered expression under high glucose treatment in endothelial cells and this is well documented [11,25]. Many genes involved in angiogenesis, the extra cellular matrix, repair and death pathways are elevated. Of particular interest to us though were the pro-inflammatory transcripts. These molecules such as IL-6, TNFα, IL-1β, and INFγ are involved in the initiation as well as sustaining an inflammatory response [13,14]. We found that the expression of these transcripts under high glucose closely matched the expression of MALAT1 in endothelial cells. Our

lab has shown previously that siRNA mediated silencing of MALAT1 prevented such upregulation of inflammatory molecules [95]. We then decided to look at MALAT1 using an animal model of diabetes to better understand its role *in vivo*. We also focused on the key process of inflammation.

To accomplish this, we obtained a MALAT1 deficient model through a collaboration with Dr. Spector [66]. This model and its development have been described previously, but briefly, it is a phenotypically normal mouse on a C57/BL6 background and is completely devoid of (lncRNA) MALAT1 in all tissues. There are no defects in breeding and the animals live past 2 years of age without intervention. The knockout was achieved with the excision of a roughly 3-kb segment that includes the MALAT1 5' promoter. Two genes which were reported to be abnormally expressed at the transcript level in both the brain cortex and liver of the animals were SAA3 and NEAT1 [66]. NEAT1 is the neighboring gene of MALAT1 and is also a lncRNA. These two molecules are both highly conserved and nearly always located side by side, despite being on different chromosomes in different species including in mouse and rat. NEAT1was found to have increased expression in the analyzed tissues in the MALAT1 knockout mouse [77]. SAA3 is a gene involved in the regulation of inflammatory molecules. It is normally expressed at high levels in the liver but in the MALAT1 knockout model, its expression was significantly decreased. This finding combined with our finding of a decreased inflammatory marker in MALAT1 KO mice, combined with our increased inflammatory markers in HG treated cells which also had increased expression of MALAT1 led us to focus on a role for the MALAT1 lncRNA in the regulation of inflammatory molecules.

We only used male mice in this study as we were not looking for gender specific differences at this time and did not want to include additional variables to the study. Diabetes was induced in animals at 10 weeks of age using STZ. We used four different time points in this study of 1, 2, 4, and 8 weeks of diabetes. Loss of MALAT1 had no effect on blood glucose levels and all groups of diabetic animals had nearly identical blood glucose levels both before and after STZ induced diabetes. Additionally, loss of

MALAT1 had no effect on polyuria or glucosuria in the diabetic animals. While diabetic, MALAT1 knockout animals did not lose the same amount of body weight as their age- sex- matched controls. We focused on the heart and kidney due to their abundant tissue supply and importance in two major diabetic complications.

MALAT1 expression in the heart and kidney tissues of WT diabetic mice was initially increased but then significantly decreased at 2, 4 and 8 weeks of diabetes. This finding was somewhat confusing. In the cell culture system, we found that high glucose caused increased MALAT1 expression in endothelial cells 48 hours after incubation with high glucose. Several possible explanations may be put forward. Tissues contain multiple cell types which interact with each other. Our initial cell culture studies were performed in HUVECS and HRECS where we showed glucose-induced MALAT1 upregulation. However, previous studies on other molecules have reported cell specific variations under the same conditions. Despite endothelial cells being the principal cell influenced by hyperglycemia, other cell types make up a larger portion of the tissues and could influence MALAT1 lncRNA levels. Moreover, direct extrapolation from cell culture in to tissue may not always be feasible. The data however, are in keeping with our array data, which showed downregulation of MALAT1 after 24 hours. Nevertheless, such an increase in MALAT1 expression in diabetes was sufficient to trigger inflammatory cytokine expression as evidenced by the inhibition of such changes in the knockout mice. It is of interest to note that in the WT diabetic mice, this initial upregulation of MALAT1 was capable of a sustained effect. The changes in MALAT1 expression from 2 to 8 weeks may indicate the possibility of a compensatory mechanism, whereby the system attempts to decrease MALAT1 expression to reduce the presence of inflammatory cytokines. An alternative possibility would be MALAT1 induction of an epigenetic regulatory change. Such a change would be inducible by the increase in MALAT1 transcript and then sustained even if MALAT1 RNA levels dropped off later [EPI]. The exact mechanism of MALAT1's regulation and action in the nucleus in producing such changes remains to be explained.

At both 1 and 2-months, inflammatory transcript levels were increased in the WT diabetic animals as was expected and has been previously reported. However, an exciting

finding was that in both heart and kidney tissues at both 1 and 2-months of diabetes, inflammatory transcript levels were not elevated at all and were maintained at WT control or even under WT control animal levels in the MALAT1 KO mice. This suggested that loss of MALAT1 had a protective effect, which inhibited the increased normally seen in diabetes.

This finding was then further supported by the examination of protein levels from 2-month animal tissues. These findings closely matched those of our transcripts where the significant increases in pro-inflammatory molecules associated with diabetes were prevented in the diabetic MALAT1 knockout animals. We further went on to look at functional differences and consequences this change in inflammatory status might have using the albumin: creatinine ratio from urine taken from the animals, and using echocardiography data that had been collected prior to sacrifice.

E/A ratio which is a measurement of left ventricular diastolic function was significantly decreased in WT diabetic animals indicating some dysfunction; however, this decrease was attenuated in the MALAT1 knockout diabetic animals again supporting our findings that the loss of MALAT1 has a protective effect. Despite this, we determined using the previously collected urine that the ACr was not significantly different between the WT and knockout diabetic animal groups. All values for albumin concentration, creatinine concentration, and 24-hour urine output were similar for the two groups leading to no significant differences between them. This suggests that the damage to the glomeruli in filtration due to diabetes may be more detrimental to the kidneys than the loss of MALAT1 can compensate for. Alternatively, MALAT1 activity may not contribute as significantly to kidney dysfunction as heart dysfunction. The differential effect of MALAT1 inhibition on renal and cardiac function may also suggest possible tissue specific pathogenetic roles of this molecule.

We also examined a few different mechanisms and interactions MALAT1 may have with other molecules. Three of these molecules were neat1, SAA3, and p53. NEAT1 is the neighboring gene of MALAT1 and changes in its expression may reflect limitations and compensations in our animal model that we need to address. In a previous

study, NEAT1 has also been shown to have a regulatory role in diabetic retinopathy [76]. As in the case of Zhang *et al*., we found NEAT1 levels to be significantly elevated in our two knockout MALAT1 mouse groups, suggesting that the molecules might regulate in –cis [66]. Neat1 expression did not however appear to change in diabetes. Neat1 has been looked at recently as a potential regulator of inflammatory molecules in cells so it is possible that MALAT1 exerts a regulatory role on NEAT1 or visa-versa. The molecules may also compensate to some degree as their functions remain largely unknown. Dual knockout MALAT1 and NEAT1 mice have not yet been attempted and may provide a phenotype which the two individual knockouts on their own seemingly lack.

MALAT1 has previously been shown to regulate SAA3 in mice, as well as inflammatory cytokines in cells induced with hyperglycemia [66,95]. Here we validate those findings but use a diabetic animal model to show that this mechanism involving MALAT1 holds true in vivo and in multiple complex organs. As with the other inflammatory molecules, SAA3 transcript expression was increased in the WT diabetic animals, and this increased expression was eliminated in both the heart and kidney tissues at both the 1 and 2-month time points.

Unlike in cancer where MALAT1 lncRNA levels are found to be at extremely high levels [76,82,87], here we have found an initial surge of MALAT1 RNA, followed by decreased expression. One reason we speculate this might be due to a compensatory mechanism where the cells attempt to decrease the amount of inflammatory cytokines being produced by reducing expression of MALAT1. Another potential mechanism involves p53 feedback which is completely absent in cancer, but found at elevated levels in diabetes. In this system, p53 appeared to be a downstream target of MALAT1. These data are in keeping with past research by other investigators. A third reason could be due to functional redundancy with other RNA transcripts such as its neighboring gene NEAT1. While we did see a decrease in inflammatory cytokine expression, it is possible other effects of the loss of MALAT1 were compensated for by other molecules. Due to its size and high basal expression levels in most tissues , the potential number of interactions MALAT1 can have is quite substantial so uncovering more about the regulatory process is essential to understanding more about MALAT1’s mechanism.

MALAT1 could also have tissue dependent functions that carry, though here we are able to show consistent suppression of inflammatory molecules in tissues that have lost MALAT1 expression.

4.1 Future Studies

Here we have identified MALAT1 as an intermediary molecule in the transcriptional pathway involved in producing inflammatory cytokines in diabetic tissues. MALAT1 is already known to be important in other diseases and pathologies, but its mechanism is largely unknown. Despite this, MALAT1 is not essential for life or development in vivo and its lack of coding potential and strong conservation between species make it a good candidate for RNA based therapies.

MALAT1 is still relatively unstudied at this point and there are many more follow-up studies need to uncover its function in diabetes, as well as in normal healthy tissues.

In this study we have shown MALAT1 is initially upregulated and then downregulated in the type-1 STZ-induced diabetic mouse model, but taking this study in to a type 2 diabetic model such as the db/db mouse, or other diabetic model would help validate our findings or even provide novel insights in MALAT1 function. Using a different animal model of diabetes might also allow us to uncover stronger associations between MALAT1 and its downstream targets. Additionally, looking at later time-points such as 4 and 6 months after the onset of diabetes would potentially be able to show a stronger protective effect on reducing inflammatory cytokines and protecting cardiac function due to the gradual progression and worsening of complications in the WT-diabetic mouse.

In this study we have focused on afflictions of the heart and kidney, but other tissues such as the retina and cerebral cortex might also provide novel insights in to the effects of MALAT1 in other tissues. We also noticed differences in the heart and kidney with respect to functional differences after the loss of MALAT1 in diabetes. Conducting cell specific studies for these tissues using podocytes or cardiomyocytes might help to understand these differences.

Whether MALAT1 lncRNA has the same effect in all tissues, or enters a tissue specific function remains unclear. Future work on the function of MALAT1 and its role in diseases like diabetes will improve our understanding of why this lncRNA has such high levels of expression and strong evolutionary conservation, potentially paving the way to new discoveries in the large family of lncRNA.

References

1. Eisenbarth, G.S., Nayak, R.C., and Rabinowe, S.L. (1988). Type I diabetes as a chronic autoimmune disease. J Diabet Complications 2, 54-58.

2. Uzzaman, A., and Cho, S.H. (2012). Chapter 28: Classification of hypersensitivity reactions. Allergy Asthma Proc *33 Suppl 1*, S96-99.

3. Palomer, X., Salvadó, L., Barroso, E., and Vázquez-Carrera, M. (2013). An overview of the crosstalk between inflammatory processes and metabolic dysregulation during diabetic cardiomyopathy. Int J Cardiol *168*, 3160-3172.

4. Shin, E.S., Sorenson, C.M., and Sheibani, N. (2014). Diabetes and retinal vascular dysfunction. J Ophthalmic Vis Res *9*, 362-373.

5. Heron, M. (2016). Deaths: Leading Causes for 2013. Natl Vital Stat Rep 65, 1-95.

6. Zhang, P., Zhang, X., Brown, J., Vistisen, D., Sicree, R., Shaw, J., and Nichols, G. (2010). Global healthcare expenditure on diabetes for 2010 and 2030. Diabetes Res ClinPract 87, 293-301.

7. Malyszko, J. (2010). Mechanism of endothelial dysfunction in chronic kidney disease. ClinChimActa 411, 1412-1420.

8. Lockhart, C.J., McCann, A.J., Pinnock, R.A., Hamilton, P.K., Harbinson, M.T., and McVeigh, G.E. (2014). Multimodal functional and anatomic imaging identifies preclinical microvascular abnormalities in type 1 diabetes mellitus. Am J Physiol Heart CircPhysiol *307*, H1729-1736.

9. Blom, M.L., Green, W.R., and Schachat, A.P. (1994). Diabetic retinopathy: a review. Del Med J *66*, 379-388.

10. Collins, A.J., Foley, R.N., Chavers, B., Gilbertson, D., Herzog, C., Johansen, K., Kasiske, B., Kutner, N., Liu, J., St Peter, W., *et al.* (2012). 'United States Renal Data System 2011 Annual Data Report: Atlas of chronic kidney disease & end-

stage renal disease in the United States. Am J Kidney Dis *59*, A7, e1-420.

11. Brownlee, M. (2001). Biochemistry and molecular cell biology of diabetic complications. Nature *414*, 813-820.

12. King, G.L., and Brownlee, M. (1996). The cellular and molecular mechanisms of diabetic complications. EndocrinolMetabClin North Am *25*, 255-270.

13. Elmarakby, A.A., Abdelsayed, R., Yao Liu, J., and Mozaffari, M.S. (2010). Inflammatory cytokines as predictive markers for early detection and progression of diabetic nephropathy. EPMA J *1*, 117-129.

14. Forbes, J.M., Fukami, K., and Cooper, M.E. (2007). Diabetic nephropathy: where hemodynamics meets metabolism. ExpClinEndocrinol Diabetes *115*, 69-84.

15. Araki, E., and Nishikawa, T. (2010). Oxidative stress: A cause and therapeutic target of diabetic complications. J Diabetes Investig 1, 90-96.

16. Cheng, H., and Harris, R.C. (2014). Renal endothelial dysfunction in diabetic nephropathy. CardiovascHematolDisord Drug Targets *14*, 22-33.

17. Giacco, F., and Brownlee, M. (2010). Oxidative stress and diabetic complications. Circ Res *107*, 1058-1070.

18. Sivitz, W.I., and Yorek, M.A. (2010). Mitochondrial dysfunction in diabetes: from molecular mechanisms to functional significance and therapeutic opportunities. Antioxid Redox Signal *12*, 537-577.

19. Keyer, K., Gort, A.S., and Imlay, J.A. (1995). Superoxide and the production of oxidative DNA damage. J Bacteriol *177*, 6782-6790.

20. Tattoli, I., Carneiro, L.A., Jéhanno, M., Magalhaes, J.G., Shu, Y., Philpott, D.J., Arnoult, D., and Girardin, S.E. (2008). NLRX1 is a mitochondrial NOD-like receptor that amplifies NF-kappaB and JNK pathways by inducing reactive oxygen species production. EMBO Rep 9, 293-300.

21. Gray, S.P., and Jandeleit-Dahm, K. (2014). The pathobiology of diabetic vascular complications--cardiovascular and kidney disease. J Mol Med (Berl) *92*, 441-452.

22. Stojceva-Taneva, O., Otovic, N.E., and Taneva, B. (2016). Prevalence of Diabetes Mellitus in Patients with Chronic Kidney Disease. Open Access Maced J Med Sci 4, 79-82.

23. Breyer, J.A., Bain, R.P., Evans, J.K., Nahman, N.S., Lewis, E.J., Cooper, M., McGill, J., and Berl, T. (1996). Predictors of the progression of renal insufficiency in patients with insulin-dependent diabetes and overt diabetic nephropathy. The Collaborative Study Group. Kidney Int *50*, 1651-1658.

24. Mora-Fernández, C., Domínguez-Pimentel, V., de Fuentes, M.M., Górriz, J.L., Martínez-Castelao, A., and Navarro-González, J.F. (2014). Diabetic kidney disease: from physiology to therapeutics. J Physiol *592*, 3997-4012.

25. Porta, M. (1996). Endothelium: the main actor in the remodelling of the retinal microvasculature in diabetes. Diabetologia 39, 739-744.

26. Singh, R., Ramasamy, K., Abraham, C., Gupta, V., and Gupta, A. (2008). Diabetic retinopathy: an update. Indian J Ophthalmol 56, 178-188.

27. Mizutani, M., Kern, T.S., and Lorenzi, M. (1996). Accelerated death of retinal microvascular cells in human and experimental diabetic retinopathy. J Clin Invest *97*, 2883-2890.

28. Akiyode, O., Major, J., and Ojo, A. (2016). Aflibercept: A Review of Its Use in the Management of Diabetic Eye Complications. J Pharm Pract.

29. Adeshara, K.A., Diwan, A.G., and Tupe, R.S. (2015). Diabetes and Complications: Cellular Signalling Pathways, Current Understanding and Targeted Therapies. Curr Drug Targets.

30. Raman, M., and Nesto, R.W. (1996). Heart disease in diabetes mellitus. EndocrinolMetabClin North Am 25, 425-438.

31. King, R.J., and Grant, P.J. (2016). Diabetes and cardiovascular disease: pathophysiology of alife-threatening epidemic. Herz *41*, 184-192.

32. Lacerda, L., Opie, L.H., and Lecour, S. (2012). Influence of tumour necrosis factor alpha on the outcome of ischaemicpostconditioning in the presence of obesity and diabetes. Exp Diabetes Res *2012*, 502654.

33. Bell, D.S. (1995). Diabetic cardiomyopathy. A unique entity or a complication of coronary artery disease? Diabetes Care *18*, 708-714.

34. Li, Z., Pearlman, A.H., and Hsieh, P. (2016). DNA mismatch repair and the DNA damage response. DNA Repair (Amst) *38*, 94-101.

35. Shimizu, I., Yoshida, Y., Suda, M., and Minamino, T. (2014). DNA damage response and metabolic disease. Cell Metab 20, 967-977.

36. Feng, B., Ruiz, M.A., and Chakrabarti, S. (2013). Oxidative-stress-induced epigenetic changes in chronic diabetic complications. Can J PhysiolPharmacol *91*, 213-220.

37. Shilatifard, A. (2006). Chromatin modifications by methylation and ubiquitination: implications in the regulation of gene expression. Annu Rev Biochem *75*, 243-269.

38. Lachner, M., Sengupta, R., Schotta, G., and Jenuwein, T. (2004). Trilogies of histone lysine methylation as epigenetic landmarks of the eukaryotic genome. Cold Spring HarbSymp Quant Biol *69*, 209-218.

39. Villeneuve, L.M., Reddy, M.A., Lanting, L.L., Wang, M., Meng, L., and Natarajan, R. (2008). Epigenetic histone H3 lysine 9 methylation in metabolic memory and inflammatory phenotype of vascular smooth muscle cells in diabetes. Proc Natl AcadSci U S A 105, 9047-9052.

40. Chen, S., Feng, B., George, B., Chakrabarti, R., Chen, M., and Chakrabarti, S. (2010). Transcriptional coactivator p300 regulates glucose-induced gene expression in endothelial cells. Am J PhysiolEndocrinolMetab 298, E127-137.

41. Lodewick, J., Lamsoul, I., Polania, A., Lebrun, S., Burny, A., Ratner, L., and Bex, F. (2009). Acetylation of the human T-cell leukemia virus type 1 Tax oncoprotein by p300 promotes activation of the NF-kappaB pathway. Virology *386*, 68-78.

42. Clark, D.W., Phang, T., Edwards, M.G., Geraci, M.W., and Gillespie, M.N. (2012). Promoter G-quadruplex sequences are targets for base oxidation and strand cleavage during hypoxia-induced transcription. Free RadicBiol Med *53*, 51-59.

43. Barres, R., and Zierath, J.R. (2011). DNA methylation in metabolic disorders. Am J ClinNutr *93*, 897S-900.

44. Wang, Z., Zheng, Y., Hou, C., Yang, L., Li, X., Lin, J., Huang, G., Lu, Q., Wang, C.Y., and Zhou, Z. (2013). DNA methylation impairs TLR9 induced Foxp3 expression by attenuating IRF-7 binding activity in fulminant type 1 diabetes. J Autoimmun *41*, 50-59.

45. Barrès, R., Osler, M.E., Yan, J., Rune, A., Fritz, T., Caidahl, K., Krook, A., and Zierath, J.R. (2009). Non-CpG methylation of the PGC-1alpha promoter through DNMT3B controls mitochondrial density. Cell Metab *10*, 189-198.

46. Liu, F., Sun, Q., Wang, L., Nie, S., and Li, J. (2015). Bioinformatics analysis of abnormal DNA methylation in muscle samples from monozygotic twins discordant for type 2 diabetes. Mol Med Rep *12*, 351-356.

47. Sassa, A., Çağlayan, M., Dyrkheeva, N.S., Beard, W.A., and Wilson, S.H. (2014). Base excision repair of tandem modifications in a methylated CpG dinucleotide. J Biol Chem*289*, 13996-14008.

48. Nakken, S., Rognes, T., and Hovig, E. (2009). The disruptive positions in human G-quadruplex motifs are less polymorphic and more conserved than their neutral counterparts. Nucleic Acids Res *37*, 5749-5756.

49. O'Hagan, H.M., Wang, W., Sen, S., Destefano Shields, C., Lee, S.S., Zhang, Y.W., Clements, E.G., Cai, Y., Van Neste, L., Easwaran, H., *et al.* (2011). Oxidative damage targets complexes containing DNA methyltransferases, SIRT1, and polycomb members to promoter CpG Islands. Cancer Cell *20*, 606-619.

50. Heneghan, H.M., Miller, N., and Kerin, M.J. (2010). Role of microRNAs in obesity and the metabolic syndrome. Obes Rev *11*, 354-361.

51. Poy, M.N., Eliasson, L., Krutzfeldt, J., Kuwajima, S., Ma, X., Macdonald, P.E., Pfeffer, S., Tuschl, T., Rajewsky, N., Rorsman, P., *et al.* (2004). A pancreatic islet-specific microRNA regulates insulin secretion. Nature *432*, 226-230.

52. Bartel, D.P. (2009). MicroRNAs: target recognition and regulatory functions. Cell *136*, 215-233.

53. Kim, V.N., Han, J., and Siomi, M.C. (2009). Biogenesis of small RNAs in animals. Nat Rev Mol Cell Biol *10*, 126-139.

54. Ben-Dov, I.Z., Tan, Y.C., Morozov, P., Wilson, P.D., Rennert, H., Blumenfeld, J.D., and Tuschl, T. (2014). Urine microRNA as potential biomarkers of autosomal dominant polycystic kidney disease progression: description of miRNA profiles at baseline. PLoS One *9*, e86856. FENG

55. Feng, B., Cao, Y., Chen, S., Chu, X., Chu, Y., and Chakrabarti, S. (2016). miR-200b Mediates Endothelial-to-Mesenchymal Transition in Diabetic Cardiomyopathy. Diabetes *65*, 768-779.

56. McArthur, K., Feng, B., Wu, Y., Chen, S., and Chakrabarti, S. (2011). MicroRNA-200b regulates vascular endothelial growth factor-mediated alterations in diabetic retinopathy. Diabetes *60*, 1314-1323.

57. Harvey, S.J., Jarad, G., Cunningham, J., Goldberg, S., Schermer, B., Harfe, B.D., McManus, M.T., Benzing, T., and Miner, J.H. (2008). Podocyte-specific deletion of dicer alters cytoskeletal dynamics and causes glomerular disease. J Am SocNephrol *19*, 2150-2158.

58. Kato, M., Arce, L., and Natarajan, R. (2009). MicroRNAs and their role in progressive kidney diseases. Clin J Am SocNephrol *4*, 1255-1266.

59. Birney, E., Stamatoyannopoulos, J.A., Dutta, A., Guigó, R., Gingeras, T.R., Margulies, E.H., Weng, Z., Snyder, M., Dermitzakis, E.T., Thurman, R.E., *et al.* (2007). Identification and analysis of functional elements in 1% of the human genome by the ENCODE pilot project. Nature *447*, 799-816.

60. Amaral, P.P., and Mattick, J.S. (2008). Noncoding RNA in development. Mamm Genome *19*, 454-492.

61. Carthew, R.W., and Sontheimer, E.J. (2009). Origins and Mechanisms of miRNAs and siRNAs. Cell *136*, 642-655.

62. Kaikkonen, M.U., Lam, M.T., and Glass, C.K. (2011). Non-coding RNAs as regulators of gene expression and epigenetics. Cardiovasc Res *90*, 430-440.

63. Shabalina, S.A., and Koonin, E.V. (2008). Origins and evolution of eukaryotic RNA interference. Trends EcolEvol *23*, 578-587.

64. Da Sacco, L., Baldassarre, A., and Masotti, A. (2012). Bioinformatics tools and novel challenges in long non-coding RNAs (lncRNAs) functional analysis. Int J MolSci *13*, 97-114.

65. Khalil, A.M., Guttman, M., Huarte, M., Garber, M., Raj, A., Rivea Morales, D., Thomas, K., Presser, A., Bernstein, B.E., van Oudenaarden, A., *et al.* (2009). Many human large intergenic noncoding RNAs associate with chromatin-modifying complexes and affect gene expression. Proc Natl AcadSci U S A *106*, 11667-11672.

66. Zhang, B., Arun, G., Mao, Y.S., Lazar, Z., Hung, G., Bhattacharjee, G., Xiao, X., Booth, C.J., Wu, J., Zhang, C., *et al.* (2012). The lncRNA Malat1 is dispensable for mouse development but its transcription plays a cis-regulatory role in the adult. Cell Rep *2*, 111-123.

67. Ma, L., Bajic, V.B., and Zhang, Z. (2013). On the classification of long non-coding RNAs. RNA Biol 10, 925-933.

68. Wilusz, J.E., Sunwoo, H., and Spector, D.L. (2009). Long noncoding RNAs: functional surprises from the RNA world. Genes Dev *23*, 1494-1504.

69. Batagov, A.O., Yarmishyn, A.A., Jenjaroenpun, P., Tan, J.Z., Nishida, Y., and Kurochkin, I.V. (2013). Role of genomic architecture in the expression dynamics of long noncoding RNAs during differentiation of human neuroblastoma cells. BMC SystBiol *7 Suppl 3*, S11.

70. He, Y., Vogelstein, B., Velculescu, V.E., Papadopoulos, N., and Kinzler, K.W. (2008). The antisense transcriptomes of human cells. Science *322*, 1855-1857.

71. Morris, K.V. (2009). Long antisense non-coding RNAs function to direct epigenetic complexes that regulate transcription in human cells. Epigenetics *4*, 296-301.

72. Mercer, T.R., Dinger, M.E., Sunkin, S.M., Mehler, M.F., and Mattick, J.S. (2008). Specific expression of long noncoding RNAs in the mouse brain. Proc Natl AcadSci U S A *105*, 716-721.

73. Wu, H., Zhao, M., Yoshimura, A., Chang, C., and Lu, Q. (2016). Critical Link Between Epigenetics and Transcription Factors in the Induction of Autoimmunity: a Comprehensive Review. Clin Rev Allergy Immunol *50*, 333-344.

74. Roberts, T.C., Morris, K.V., and Weinberg, M.S. (2014). Perspectives on the mechanism of transcriptional regulation by long non-coding RNAs. Epigenetics *9*, 13-20.

75. Ji, P., Diederichs, S., Wang, W., Böing, S., Metzger, R., Schneider, P.M., Tidow, N., Brandt, B., Buerger, H., Bulk, E., *et al.* (2003). MALAT-1, a novel noncoding RNA, and thymosin beta4 predict metastasis and survival in early-stage non-small cell lung cancer. Oncogene *22*, 8031-8041.

76. Li, T., Mo, X., Fu, L., Xiao, B., and Guo, J. (2016). Molecular mechanisms of long noncoding RNAs on gastric cancer. Oncotarget *7*, 8601-8612.

77. Ulitsky, I., Shkumatava, A., Jan, C.H., Sive, H., and Bartel, D.P. (2011). Conserved function of lincRNAs in vertebrate embryonic development despite rapid sequence evolution. Cell *147*, 1537-1550.

78. Han, P., Li, W., Lin, C.H., Yang, J., Shang, C., Nurnberg, S.T., Jin, K.K., Xu, W., Lin, C.Y., Lin, C.J., *et al.* (2014). A long noncoding RNA protects the heart from pathological hypertrophy. Nature *514*, 102-106.

79. Gast, M., Schroen, B., Voigt, A., Haas, J., Kuehl, U., Lassner, D., Skurk, C., Escher, F., Wang, X., Kratzer, A., *et al.* (2016). Long noncoding RNA MALAT1-derived mascRNA is involved in cardiovascular innate immunity. J Mol Cell Biol *8*, 178-181.

80. Akkuratov, E.E., Walters, L., Saha-Mandal, A., Khandekar, S., Crawford, E., Zirbel, C.L., Leisner, S., Prakash, A., Fedorova, L., and Fedorov, A. (2014). Bioinformatics analysis of plant orthologous introns: identification of an intronictRNA-like sequence. Gene *548*, 81-90.

81. Johnsson, P., Lipovich, L., Grandér, D., and Morris, K.V. (2014). Evolutionary conservation of long non-coding RNAs; sequence, structure, function. BiochimBiophysActa *1840*, 1063-1071.

82. Tani, H., Nakamura, Y., Ijiri, K., and Akimitsu, N. (2010). Stability of MALAT-1, a nuclear long non-coding RNA in mammalian cells, varies in various cancer cells. Drug DiscovTher *4*, 235-239.

83. Brown, J.A., Valenstein, M.L., Yario, T.A., Tycowski, K.T., and Steitz, J.A. (2012). Formation of triple-helical structures by the 3'-end sequences of MALAT1 and MENβ noncoding RNAs. Proc Natl AcadSci U S A *109*, 19202-19207.

84. Xu, C., Yang, M., Tian, J., Wang, X., and Li, Z. (2011). MALAT-1: a long non-coding RNA and its important 3' end functional motif in colorectal cancer metastasis. Int J Oncol *39*, 169-175.

85. Gutschner, T., Baas, M., and Diederichs, S. (2011). Noncoding RNA gene silencing through genomic integration of RNA destabilizing elements using zinc finger nucleases. Genome Res *21*, 1944-1954.

86. Eißmann, M., Gutschner, T., Hämmerle, M., Günther, S., Caudron-Herger, M., Groß, M., Schirmacher, P., Rippe, K., Braun, T., Zörnig, M., *et al.* (2012). Loss of the abundant nuclear non-coding RNA MALAT1 is compatible with life and development. RNA Biol *9*, 1076-1087.

87. Luo, J.H., Ren, B., Keryanov, S., Tseng, G.C., Rao, U.N., Monga, S.P., Strom, S., Demetris, A.J., Nalesnik, M., Yu, Y.P., *et al.* (2006). Transcriptomic and genomic analysis of human hepatocellular carcinomas and hepatoblastomas. Hepatology *44*, 1012-1024.

88. Rajaram, V., Knezevich, S., Bove, K.E., Perry, A., and Pfeifer, J.D. (2007). DNA sequence of the translocation breakpoints in undifferentiated embryonal sarcoma arising in mesenchymal hamartoma of the liver harboring the t(11;19)(q11;q13.4) translocation. Genes Chromosomes Cancer *46*, 508-513.

89. Lai, M.C., Yang, Z., Zhou, L., Zhu, Q.Q., Xie, H.Y., Zhang, F., Wu, L.M., Chen, L.M., and Zheng, S.S. (2012). Long non-coding RNA MALAT-1 overexpression predicts tumor recurrence of hepatocellular carcinoma after liver transplantation. Med Oncol *29*, 1810-1816.

90. Mohamadkhani, A. (2014). Long Noncoding RNAs in Interaction With RNA Binding Proteins in Hepatocellular Carcinoma. Hepat Mon *14*, e18794.

91. Kryger, R., Fan, L., Wilce, P.A., and Jaquet, V. (2012). MALAT-1, a non protein-coding RNA is upregulated in the cerebellum, hippocampus and brain stem of human alcoholics. Alcohol *46*, 629-634.

92. Ma, X.Y., Wang, J.H., Wang, J.L., Ma, C.X., Wang, X.C., and Liu, F.S. (2015). Malat1 as an evolutionarily conserved lncRNA, plays a positive role in regulating proliferation and maintaining undifferentiated status of early-stage hematopoietic cells. BMC Genomics *16*, 676.

93. Tripathi, V., Shen, Z., Chakraborty, A., Giri, S., Freier, S.M., Wu, X., Zhang, Y., Gorospe, M., Prasanth, S.G., Lal, A., *et al.* (2013). Long noncoding RNA MALAT1 controls cell cycle progression by regulating the expression of oncogenic transcription factor B-MYB. PLoS Genet *9*, e1003368.

94. Yang, S., Yao, H., Li, M., Li, H., and Wang, F. (2016). Long Non-Coding RNA MALAT1 Mediates Transforming Growth Factor Beta1-Induced Epithelial-Mesenchymal Transition of Retinal Pigment Epithelial Cells. PLoS One *11*, e0152687.

95. Puthanveetil, P., Chen, S., Feng, B., Gautam, A., and Chakrabarti, S. (2015). Long non-coding RNA MALAT1 regulates hyperglycaemia induced inflammatory process in the endothelial cells. J Cell Mol Med *19*, 1418-1425.

96. Gast, M., Schroen, B., Voigt, A., Haas, J., Kuehl, U., Lassner, D., Skurk, C., Escher, F., Wang, X., Kratzer, A., *et al.* (2016). Long noncoding RNA MALAT1-derived mascRNA is involved in cardiovascular innate immunity. J Mol Cell Biol *8*, 178-181.

97. Feng, B., Chen, S., George, B., Feng, Q., and Chakrabarti, S. (2010). miR133a regulates cardiomyocyte hypertrophy in diabetes. Diabetes Metab Res Rev *26*, 40-49.

98. Chen, S., Khan, Z.A., Cukiernik, M., and Chakrabarti, S. (2003). Differential activation of NF-kappa B and AP-1 in increased fibronectin synthesis in target organs of diabetic complications. Am J PhysiolEndocrinolMetab *284*, E1089-1097.

99. Coassin, S.R., Orjalo, A.V., Semaan, S.J., and Johansson, H.E. (2014). Simultaneous detection of nuclear and cytoplasmic RNA variants utilizing Stellaris® RNA fluorescence in situ hybridization in adherent cells. Methods MolBiol 1211, 189-199.

100. Pistner, A., Belmonte, S., Coulthard, T., and Blaxall, B. (2010). Murine echocardiography and ultrasound imaging. J Vis Exp.

101. Lin, M.F., Jungreis, I., and Kellis, M. (2011). PhyloCSF: a comparative genomics method to distinguish protein coding and non-coding regions. Bioinformatics 27, i275-282.

102. Hung, T., Wang, Y., Lin, M.F., Koegel, A.K., Kotake, Y., Grant, G.D., Horlings, H.M., Shah, N., Umbricht, C., Wang, P., et al. (2011). Extensive and coordinated transcription of noncoding RNAs within cell-cycle promoters. Nat Genet 43, 621-629.

103. Oviedo-Socarrás, T., Vasconcelos, A.C., Barbosa, I.X., Pereira, N.B., Campos, P.P., and Andrade, S.P. (2014). Diabetes alters inflammation, angiogenesis, and fibrogenesis in intraperitoneal implants in rats. Microvasc Res 93, 23-29.

104. Shelbaya, S., Amer, H., Seddik, S., Allah, A.A., Sabry, I.M., Mohamed, T., and El Mosely, M. (2012). Study of the role of interleukin-6 and highly sensitive C-reactive protein in diabetic nephropathy in type 1 diabetic patients. Eur Rev Med PharmacolSci 16, 176-182.

105. Navarro-González, J.F., Mora-Fernández, C., Muros de Fuentes, M., and García-Pérez, J. (2011). Inflammatory molecules and pathways in the pathogenesis of diabetic nephropathy. Nat Rev Nephrol 7, 327-340.

106. Hara, T., Ishida, T., Cangara, H.M., and Hirata, K. (2009). Endothelial cell-selective adhesion molecule regulates albuminuria in diabetic nephropathy. Microvasc Res 77, 348-355.

107. Chang, J.H., Paik, S.Y., Mao, L., Eisner, W., Flannery, P.J., Wang, L., Tang, Y., Mattocks, N., Hadjadj, S., Goujon, J.M., et al. (2012). Diabetic kidney disease in FVB/NJ Akita mice: temporal pattern of kidney injury and urinary nephrin excretion. PLoS One 7, e33942.

108. Doi, T., Mima, A., Matsubara, T., Tominaga, T., Arai, H., and Abe, H. (2008). The current clinical problems for early phase of diabetic nephropathy and approach for pathogenesis of diabetic nephropathy. Diabetes Res ClinPract 82 Suppl 1, S21-24.

109. Schutte, J.E., Longhurst, J.C., Gaffney, F.A., Bastian, B.C., and Blomqvist, C.G. (1981). Total plasma creatinine: an accurate measure of total striated muscle mass. J ApplPhysiolRespir Environ ExercPhysiol 51, 762-766.

110. Harita, N., Hayashi, T., Sato, K.K., Nakamura, Y., Yoneda, T., Endo, G., and Kambe, H. (2009). Lower serum creatinine is a new risk factor of type 2 diabetes: the Kansai healthcare study. Diabetes Care 32, 424-426.

111. Jardine, M.J., Hata, J., Woodward, M., Perkovic, V., Ninomiya, T., Arima, H., Zoungas, S., Cass, A., Patel, A., Marre, M., *et al.* (2012). Prediction of kidney-related outcomes in patients with type 2 diabetes. Am J Kidney Dis *60*, 770-778.

112. Atas, H., Kepez, A., Atas, D.B., Kanar, B.G., Dervisova, R., Kivrak, T., and Tigen, M.K. (2014). Effects of diabetes mellitus on left atrial volume and functions in normotensive patients without symptomatic cardiovascular disease. J Diabetes Complications *28*, 858-862.

Curriculum Vitae

Name:	Andrew Gordon
Post-secondary Education and Degrees:	Western University London, Ontario, Canada 2010-2014 B.Sc.
Honours and Awards:	Western Graduate Research Scholarship 2014-2016
Related Work Experience	Teaching Assistant Western University 2015-2016

Publications: Feng, B., Chen, S., Gordon, A., Chakrabarti, S. (2016). miR-146a mediates inflammatory changes and fibrosis in the heart in diabetes. Diabetologia. (Submitted).